



HAL
open science

Analyse des incertitudes dans les flux du trafic aérien.

Claus Gwiggner

► **To cite this version:**

Claus Gwiggner. Analyse des incertitudes dans les flux du trafic aérien.. Informatique [cs]. Ecole Polytechnique X, 2007. Français. NNT: . pastel-00003211

HAL Id: pastel-00003211

<https://pastel.hal.science/pastel-00003211>

Submitted on 27 Jul 2010

HAL is a multi-disciplinary open access archive for the deposit and dissemination of scientific research documents, whether they are published or not. The documents may come from teaching and research institutions in France or abroad, or from public or private research centers.

L'archive ouverte pluridisciplinaire **HAL**, est destinée au dépôt et à la diffusion de documents scientifiques de niveau recherche, publiés ou non, émanant des établissements d'enseignement et de recherche français ou étrangers, des laboratoires publics ou privés.

Thèse présentée pour obtenir le grade de
DOCTEUR DE L'ÉCOLE POLYTECHNIQUE
Spécialité: Informatique

**ANALYSE DES INCERTITUDES DANS LES
FLUX DU TRAFIC AÉRIEN**
ANALYSIS OF UNCERTAINTIES IN AIR-TRAFFIC FLOW

par

Claus Peter GWIGNER

Soutenue le 13 septembre 2007 après avis de:

Nicolas DURAND (Rapporteur)
John HANSMAN (Rapporteur)

devant le jury composé de:

Philippe BAPTISTE (Directeur de thèse)
Pierre COLLET
Vu DUONG (Directeur de thèse)
Jean-Marie MARION
Jean-Marc STEYAERT (Président)

Remerciements

Je tiens à remercier Monsieur Philippe Baptiste et Monsieur Vu Duong d'avoir accepté d'encadrer cette thèse. Leurs intuitions m'ont sans cesse laissé grandir, que ce soit sur la nature d'un modèle ('comment en choisir un?') ou sur l'inférence ('c'est juste un outil'). Mais le plus important est qu'ils m'ont encouragé à trouver et poursuivre mes propres intérêts de recherche.

Pendant cette thèse j'ai eu la chance de collaborer avec des chercheurs qui ont élargi mon horizon. Monsieur Pierre Collet a répondu avec patience à toutes mes questions et m'a silencieusement guidé vers les aspects fondamentaux de l'aléatoire. Ainsi que Monsieur Jean-Marie Marion, qui m'a montré comment adopter une attitude rigoureuse envers l'inférence statistique.

Ce fut un honneur pour moi que Monsieur Nicolas Durand et Monsieur John Hansman aient accepté d'être rapporteurs de cette thèse et Monsieur Jean-Marc Steyaert d'en être le président de la jury.

Je remercie Monsieur Christophe Dürr et Monsieur James Lindsey pour avoir relu le manuscrit de thèse et pour avoir partagé leurs raisonnements purs avec moi. Je remercie également Monsieur Leo Liberti pour son ouverture d'esprit.

Merci beaucoup à Madame Kerstin Schill qui m'a prêté avec sagesse certains choix qu'il fallait faire en tant que thésard.

Merci aussi aux membres du groupe Ino du Centre Expérimental de Eurocontrol et du Laboratoire d'Informatique de l'École polytechnique. En particulier à mes collègues de bureau Antonia, Fred, Lisa, Mathilde, Monica, Olivier, Thang et Xavier qui m'ont donné des bonnes raisons d'y revenir jour par jour.

Enfin, je remercie mes amis et ma famille pour m'avoir donné la confiance de mener cette thèse en toute intégrité.

Résumé

La gestion du trafic aérien (air-traffic management, ATM) consiste en une composante prédictive (planification du trafic) et en une composante adaptative (contrôle du trafic). Le but de la composante prédictive est de trouver un équilibre entre la demande de l'espace et la capacité disponible. Une fois que les avions ont décollé, la composante adaptative doit les guider en toute sécurité vers leurs destinations. Des incertitudes, telles que retards ou défaillances techniques, créent des phénomènes d'écarts entre la composante prédictive et adaptative. Cela entraîne des problèmes de sécurité ainsi qu'une utilisation sous-optimale de capacité. Même si les causes majeures des incertitudes sont connues (incertitude de demande, incertitude de capacité, incertitude de gestion de flux), les mécanismes perturbateurs restent inconnus.

L'approche de cette thèse est d'analyser des données d'écoulement de trafic afin d'engendrer de nouvelles hypothèses sur les mécanismes qui causent des écarts entre la composante prédictive et adaptative dans l'ATM. C'est un premier pas pragmatique dans l'analyse d'un phénomène physique. Il est fondé sur le calcul des probabilités et plus précisément sur l'interprétation fréquentiste des probabilités. On utilise des techniques d'analyse de données multi-variées et des processus ponctuels stochastiques afin d'inférer de nouvelles connaissances sur le phénomène.

Nos résultats principaux sont:

- (i) des écarts systématiques existent dans tous les secteurs évalués. Leur taille peut être caractérisée par des distributions de Poisson et on constate une tendance systématique à supprimer le trafic sur des niveaux élevés de planification. C'est un résultat contre-intuitif car l'on s'attend à ce que les différents facteurs d'incertitude s'annulent en moyenne. Ensuite on montre que des perturbations aléatoires d'un processus d'arrivée causent des écarts systématiques dans deux classes de plan de vol. On conclut que même si toutes les incertitudes contrôlables étaient éliminées, des écarts systématiques entre le nombre planifié et observé de vols apparaîtraient. Ce résultat est utile pour la planification tactique des flux. De nouvelles contraintes pour le problème de l'allocation de créneaux peuvent être formulées en identifiant des plans de vol qui sont robustes aux perturbations aléatoires.
- (ii) on montre que les écarts se propagent uniquement le long des routes aériennes. Aucune propagation non-attendue n'est identifiée. Cela indique que les contrôleurs aériens n'utilisent pas systématiquement le reroutage pour compenser les écarts. On remarque également des probabilités de queue élevées et on propose deux (nouveaux) modèles de séries chronologiques qui décrivent les caractéristiques du processus de pertur-

bation des plans de vol. Cela indique que les perturbations sont d'une nature hétérogène et non-indépendante. Le résultat est empirique et on affirme que le comportement observé est du à des dépendances entre les avions intervenant sur un long-terme.

Comme travaux futurs on propose de continuer l'identification des ordonnancements de vol qui absorbent l'impact des incertitudes non-contrôlables et de développer des modèles statistiques qui expliquent les échantillons long-terme de congestion. Ceci constitue une base pour la quantification de l'impact des décisions locales sur la performance globale du réseau de transport.

Abstract

Air-traffic management (ATM) consists of a predictive component (traffic planning) and an adaptive component (traffic control). The aim of the predictive component is to balance airspace demand with available capacity. The adaptive component has to guide aircraft safely to their destinations, once they are in the air. Uncertainties (e.g delay from connecting flights, technical failure) create the phenomenon of gaps between the predictive and the adaptive component. This causes safety problems and non-optimally used capacity. While the main sources of uncertainties are identified (demand uncertainties, capacity uncertainties, flow control uncertainties) the mechanisms of how they affect the components of air-traffic management remain unknown.

Our approach is to analyze past flight data to *generate hypotheses* about the mechanisms that lead to gaps between the predictive and the adaptive component in ATM. This is a pragmatic first step in the analysis of a physical phenomenon. It is based on probability theory and more precisely on a frequentist interpretation of uncertainty. We use multivariate data analysis techniques and stochastic Point processes to infer new knowledge about the phenomenon.

Our main results are

- (i) there are *systematic* gaps in each sector evaluated. The size of these gaps can be characterized by Poisson distributions and there is a systematic shift to suppress traffic at high planned levels. This is counter-intuitive because one expects that the different uncertainty factors cancel out in average. We then prove that random disturbances of an arrival process cause systematic gaps in two classes of flight schedules. We conclude that even if all controllable uncertainties in flow planning were eliminated, systematic gaps between the number of planned and realized traffic would remain. This result is useful in tactical flow planning. New constraints in the slot-allocation procedure can be found by identifying classes of flight schedules that are robust to random disturbance.
- (ii) we show that gaps propagate exclusively on flight routes. No unexpected propagation is identified. This is evidence that no systematic re-routing is initiated by controllers to absorb gaps. We also identify high tail probabilities and two time-series models which describe the second-order characteristics of the process that disturbs the flight schedules. This is evidence that the disturbances are heterogeneous and not independent. This result is empirical and we conjecture that the observed behavior is due to aggregation and long-range dependence at the sector level.

As future work we propose to continue the identification of classes of flight schedules that absorb the impact of uncontrollable disturbances and to develop

statistical models that explain long-term congestion patterns. This is a basis to quantify the impact of local decisions on the performance of the global sector network.

Contents

Remerciements	2
Résumé	3
Abstract	5
Table of Contents	3
Notation	9
1 Introduction	11
1.1 Uncertainties in Air-Traffic Flow Management	11
Components of traffic management	12
Current limitations	14
Uncertainties	14
Gaps between planned and realized traffic	15
1.2 Data Analysis and Uncertainty	16
Formalisms	16
Interpretation(s) of probability	16
1.3 Methodology	18
Possible approaches	18
Position of the thesis	19
1.4 Thesis Outline	20
Main objectives	20
Approach	20
Thesis structure	20
2 Background and Data Description	23
2.1 Random vectors	23
Independence	25
Correlation	25
2.2 Likelihood	27
Likelihood function	27
Parameter estimation	28
2.3 Examples from Multivariate Data Analysis	29

Open-loop systems	29
Multivariate time-series	29
Graphical models	30
2.4 Data Description	31
Format and type	31
Period	32
Geographic area	33
Quality	33
3 Results of Exploratory Analysis	35
Description of gaps	35
Methodology	36
Formalization	36
Related work	36
Plan of the chapter	37
3.1 Summary of Results	38
Uncertainty of gaps	38
Systematic gaps between planned and realized	38
Propagation of gaps	38
3.2 Uncertainty of Gaps	39
Absolute	41
Relative	42
Functional	44
3.3 Occurrence of Gaps	48
Function of time	48
Function of planned traffic	49
3.4 Propagation of Gaps	52
Visualization	52
Inference for correlation matrices	53
Results	59
3.5 Validation	67
Aggregation	67
Generalization	67
3.6 Interpretation	70
Uncertainty	70
Occurrence	71
Propagation	71
Conclusion	71
4 Results of Probabilistic Analysis	73
Mechanisms of gaps	73
Methodology	75
Formalization	75
Related work	75
Chapter outline	76
4.1 Summary of Results	77

Complete random disturbances cause gaps	77
Real disturbances do not occur at random	77
4.2 Consequences of Independence Assumptions	78
Point processes	78
Operations on Point processes	78
Analytical results	81
Proof of proposition 4.2.4	83
Experimental results	85
Interpretation	87
4.3 Dependency Structure of Disturbances	88
Flow structure	88
Shapes of decaying autocorrelation	88
Dependency structure of disturbances	90
4.4 Interpretation	93
5 Conclusions and Future Work	97
5.1 Summary of contributions	97
5.2 Perspectives	98
Bibliography	106

List of Figures

1.1	Sector and route network	12
1.2	Flow planning process	13
1.3	Flow planning and flow control	14
1.4	Impact of uncertainties	15
1.5	Sample trajectory of a random walk	17
2.1	Undirected graphical model	30
2.2	Central European airspace	32
2.3	Traffic statistics	33
3.1	Time plots	40
3.2	Sample autocorrelation functions	41
3.3	Absolute gaps	42
3.4	QQ plot	43
3.5	Relative gaps	44
3.6	QQ plot	45
3.7	Functional gaps	46
3.8	Daily arrival pattern	49
3.9	Fundamental scatterplot	50
3.10	Fundamental relationship	51
3.11	30 minutes evolution of traffic	54
3.12	Cross-correlation matrix (visualization)	60
3.13	Cross-correlation matrix (local)	61
3.14	Cross-correlation matrix (global)	62
3.15	Scatterplot	63
3.16	Summaries of correlation	64
3.17	Strength of correlation	65
3.18	Distribution of correlation	66
3.19	Time-scales	68
3.20	Sample means	69
4.1	Events at a sector entry	74
4.2	Consequences of independence assumption	82
4.3	Randomly disturbed Point processes	82

4.4	Empirical distribution of disturbances	86
4.5	Time plot	90
4.6	Sample acf and pacf	91
4.7	Length of correlated arrival sequences	93
4.8	Diagnostics for ARMA(1,1) model	95
4.9	QQ plot	96
4.10	Lag plot	96

List of Tables

3.1	Marginal distribution of absolute gaps	43
3.2	Marginal distribution of relative gaps	44
3.3	Goodness-of-fit of Poisson and Binomial model	46
3.4	Goodness-of-fit of different trend models	52
4.1	Simulation of 12 randomly selected sectors	85
4.2	Comparison ARMA(1,1) and IMA(1,1)	93
4.3	Comparison ARMA(1,1) IMA(1,1)	94
4.4	Validation ARMA(1,1)	94

Notation

Notation	Description
ATM	air traffic management.
CASA	Computer Aided Slot Allocation.
flight plan	sequence $(S_1, t_1), \dots, (S_n, t_n)$ of sectors S_i and of estimated entry time points t_i .
initial demand	the flight plans before regulation.
regulated demand	the flight plans after regulation.
observed demand	the flight plans flown in reality.
uncertainty factor	event that disturbs flight plans.
GAP	difference between observed and regulated demand.
$\mathbf{X}=(X_1, \dots, X_n)$	random vector.
$P_X(x_1, \dots, x_n)$	Joint probability distribution.
$P_{X_i}(x_i)$	marginal probability distribution.
$P_{Y X}(y x)$	conditional probability distribution.
$L_\theta(x_1, \dots, x_n)$	likelihood function.
$\mathbf{E}(\mathbf{X})$	expectation.
$\mathbf{E}(\mathbf{X} \mathbf{Y})$	conditional expectation.
$\Sigma_{\mathbf{X}}(k)$	covariance matrix function.
$\rho_{\mathbf{X}}(k)$	correlation matrix function.
$\{\tau_i\}, \tau_i \in \mathbb{R}, i \in \mathbb{Z}$	planned arrival process.
$\{\tau'_i\}, \tau'_i \in \mathbb{R}, i \in \mathbb{Z}$	observed arrival process.
$\{\epsilon_i\}, \epsilon_i \in \mathbb{R}, i \in \mathbb{Z}$	disturbance process.

Chapter 1

Introduction

Air transportation is an area in which safety has the highest priorities. Every accident has a world-wide amplitude and questions the reliability of the actors of the air transportation industry: the constructors (the Concorde accident, 2000), the control system (lake Constance, 2002) or the airline companies (Charm el Cheikh, 2004). The today's standard in air transportation is based on strict security rules. The definition of these rules and the control of their application is under the responsibility of the International Civil Aviation Organization (ICAO). Other requirements in air transportation include the respect of the environment and cost-efficiency [ICAO, 2005], [EUROCONTROL, 2006]. All requirements concern every actor and have to be re-evaluated permanently due to a dynamically growing market. Eurocontrol, the European Organization for the Safety of Air Navigation, develops strategies to meet these requirements. Its research center accommodates the departments applied (short-, medium-, long-term) and innovative research. The latter's mission is to undertake experimental studies as candidates for further investigation in one of the applied branches. Examples are models for complex systems and for uncertainty in traffic flow management [EUROCONTROL, 2005].

1.1 Uncertainties in Air-Traffic Flow Management

In this thesis we consider air transportation as a *system* consisting of several components such as airports, airlines and traffic flow management. These components have different objectives; for example airlines wish to optimize their fleet-schedules and airports the runway capacities; but they share the same resource: the airspace. The airspace is a network of sectors and routes. Sectors are geographical regions and routes connect sectors. Figure 1.1 shows the sector - and route network above central Europe. The yellow routes are directed from north to south and the brown routes in the opposite direction. One can see a high route density and major axes between London-Frankfurt and Berlin-

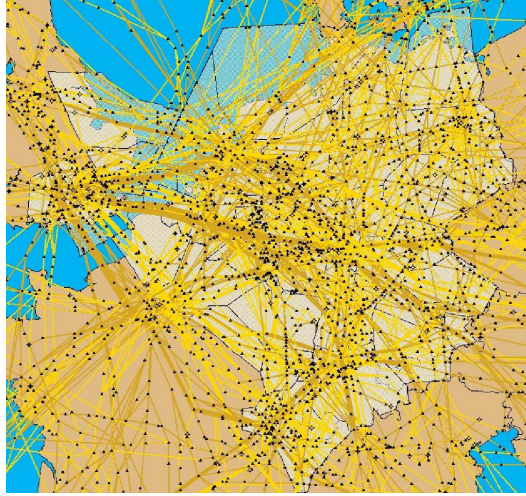


Figure 1.1: Sector and route network (central Europe).

Paris. Currently more than 1500 sectors and more than 50.000 routes build the transportation network, serving more than 22.000 daily flights to take place [EUROCONTROL, 2006].

Components of traffic management

The goal of the air traffic management component (ATM) is to achieve safe, orderly, and economic flows of traffic [EUROCONTROL, 1997]. It consists of the two sub-components *flow planning* and *flow control*. Flow planning takes place before take-off and flow control during the flight. Figure 1.2 shows the scope of flow planning. It is a long-term process, ranging from research on new sector- and route designs (strategic phase) over the analysis of flow patterns (pre-tactical phase) until the daily schedule of departure slots to avoid congestion (tactical phase). The mission of flow planning is to balance airspace demand with available capacity. It is a centralized service which has to anticipate the future evolution of the network. For this reason, we call it the *predictive component* in traffic management.

Example: Computer Aided Slot Allocation (CASA). On a daily basis, departure slots are distributed amongst aircraft to respect sector capacities. Capacity is defined as the maximum number of aircraft that are allowed to enter a sector during one hour. The procedure is that airlines submit flight plans at least two hours before the intended take-off time to the flow-planning center. A flight plan is a sequence $(S_1, t_1), \dots, (S_n, t_n)$ of sectors S_i and of estimated entry time points t_i , following the pre-defined routes. Based on this information, take-off times $t'_1 \geq t_1$ of aircraft are calculated that (i) respect all sector capacities and

strategic	pre-tactical	tactical
<ul style="list-style-type: none"> • network evolution • demand evolution • capacity evolution 	<ul style="list-style-type: none"> • flow pattern analysis • re-routing • regulation plan 	<ul style="list-style-type: none"> • slot allocation • ad-hoc re-routing
long-term	one week ahead	day d

Figure 1.2: Flow planning process

(ii) minimize the total delay of the individual aircraft.

Once an aircraft is in the air, traffic controllers guide it from origin to destination. Each sector is directly supervised by two controllers, one in charge of conflict detection, and the other in charge of conflict resolution. Minimum distances between aircraft have to be kept. This is achieved by re-routing and speed adjustments. Behind this direct control of aircraft, an organizational effort can be found. Sectors belong to flow centers. There are currently 75 flow centers in the European airspace. In each flow center, flow managers analyze the traffic flows and make traffic predictions. They combine several information sources for this: radar data, weather forecast, abnormal events at airports, and so on. Based on their prediction of the real traffic situation they can initiate several actions. For example they can divide sectors into smaller units to answer to high traffic peaks, they can coordinate re-routing of whole flows with other flow managers or they can declare temporal capacity constraints to the flow planning center. The difference to flow planning is that flow control adapts its behavior to the real traffic situation. For this reason we call it the *adaptive component* in traffic management.

Example: Dynamic CASA. A flow manager predicts an unusual traffic peak in one of his sectors for the afternoon because a storm will lead pilots to avoid a neighboring sector. He calls the flow managers from the neighboring centers by telephone to find a way to re-route the aircraft over the network. Two hours before the beginning of the storm, he communicates a temporary capacity limitation for his sectors to the flow planning center.

The link between flow planning and flow control in the pre-tactical and tactical phase is shown in Figure 1.3. Flow planning has to guarantee that sector capacities are never exceeded. This is done by re-routing and slot allocation. Re-routing is currently a manual procedure while slot allocation is done automatically. And flow control has to provide capacities that allow for an efficient usage of the airspace. This is done by declaration of appropriate capacities and by re-sectorizations; both are inputs to the flow planning component.

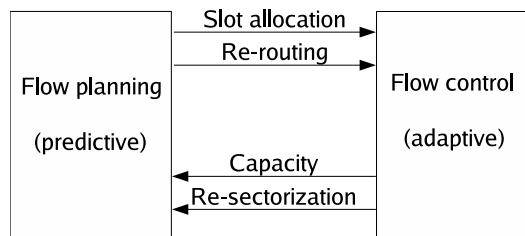


Figure 1.3: Link between flow planning and flow control in tactical and pre-tactical phase

Current limitations

A main limitation of flow planning is that trajectory and speed of aircraft are assumed to be known in advance. In reality, *uncertainty* about the behavior of airspace users, e.g. passenger delays, controller and pilots behavior or about weather conditions disturb the flight plans. For example in the year 2004, 17.7 % of the flights departed- and 18.5 % arrived more than 15 min behind their schedule [EUROCONTROL, 2006].

Uncertainties

[Ball et al., 2005] classify the major sources of uncertainty as

- Demand uncertainty: flights fail to meet planned departure, arrival or en-route travel times. Contributing factors are mechanical problems, boarding passengers or weather conditions.
- Capacity uncertainty: airport and airspace throughput levels vary. Contributing factors are weather conditions and changes in flight sequences that disturb scheduled departure or arrival spacing.
- Flow control uncertainty: actions are taken by the traffic controllers in response to demand and capacity uncertainty. Examples are re-routing, re-sectorization and temporary capacity limitations. The human element of decision making adds another layer of uncertainty to the whole system.

Example: Reactionary Delay. Reactionary delay is caused by late arrival of an aircraft or the crew from connecting flights. This delay is propagated through the whole sector network because (i) aircraft generally fly the same route several times a day and (ii) connecting flights generally have to wait for delayed flights. Reactionary delay is the largest single delay factor in the European airspace. In 2004, it accounted for 39.5 % of all delayed flights. Its portion is increasing during the last years. Currently, it is not known how the local decisions of airlines, airport or ATM affect this delay propagation [EUROCONTROL, 2006].

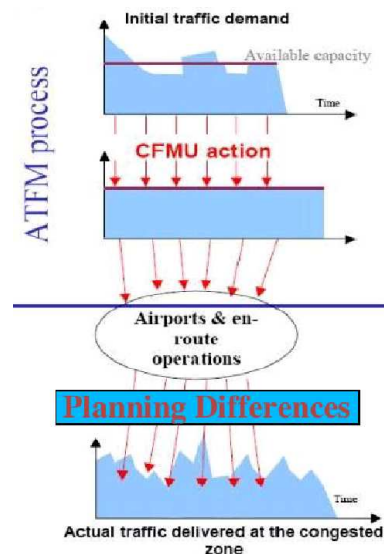


Figure 1.4: Consequences of uncertainties on sector level

Gaps between planned and realized traffic

Figure 1.4 shows the consequences of uncertainties in flow planning on a sector level. During flow planning, the initial demand is transformed into regulated demand such that all sector capacities are satisfied (top and middle). Uncertainties that have not been taken into account in the regulation translate into gaps between the planned number and the realized number of aircraft arriving at sectors (bottom). This leads to safety problems and non-optimally used capacity. For example during the last years, situations in which the actual demand is more than 10 % greater than the capacity occurred in 10 % the time [EUROCONTROL, 2006].

As a whole, the components of airspace build a socio-technical system. Controllers and pilots frequently make decisions based on uncertain or incomplete information. The nature of these uncertainties and its impact on the flow management process is currently badly understood [EUROCONTROL, 2002], [EUROCONTROL, 2006]. Interdisciplinary research is done towards a better understanding of the impact of uncertainty on flow management. The aim is to close the gap between the predictive and adaptive components of flow management. This is a basis for a safe, efficient and sustainable usage of the resource ‘airspace’.

1.2 Data Analysis and Uncertainty

One scientific view of the world is that nature makes no arbitrary choices. Randomness is the result of incomplete or erroneous information. For example in mechanics, the trajectory of objects can be described exactly from basic principles. Uncertainty in the observations of the objects and the environmental conditions is often called ‘measurement error’. The other view states that it is impossible to obtain complete information about an object. For example living organisms may behave differently under identical conditions. Assuming deterministic behavior is unrealistic, and any model of the individuals behavior has to include a stochastic part. This type of uncertainty is called ‘intrinsic uncertainty’ [Lindsey, 2003]. In both cases, measurement errors and intrinsic uncertainty lead to *variation* in observed variables that asks to be understood and to be quantified.

Example: Random walk. Figure 1.5 shows a sample trajectory of the model

$$y_t = y_{t-1} + \epsilon_t$$

where ϵ is a random variable with zero mean, and values ϵ_t, ϵ_s are uncorrelated for $t \neq s$. It shows oscillatory behavior, increasing in the beginning, falling down in the second third and increasing then, again. One could be tempted to model the trajectory as a deterministic function of time subject to measurement errors. This assumption would lead to wrong physical interpretations.

Formalisms

Several formalisms to model uncertainty have been developed. The most widely known is probability theory [Kolmogoroff, 1933]. Others are the theory of fuzzy sets [Zadeh, 1965] and possibility theory [Zadeh, 1978]. As to date, probability theory is the formalism with the best understood foundations.

Interpretation(s) of probability

Probability theory is an axiomatic theory, allowing to deduce probabilistic statements from previously stated premises. There is universal agreement on this [Cox and Snell, 1981], [Chatterjee, 2003], [Saporta, 2006]. For example, we will proof in chapter 4 that when the arrival process at a sector entry is a randomly disturbed Poisson process, the average size of gaps is > 0 for low traffic densities and < 0 for high traffic densities. Concerning the meaning of ‘probability’, there is less agreement. A study of the philosophy of probability theory shows a controversial discussion about the interpretation of ‘probability’ [Chatterjee, 2003], [Lindsey, 2003], [Cox, 2006]. Two schools of thought are

- **Frequentist.** Probability is defined as limiting proportion of times that an event would occur in repetitions of a random experiment under identical conditions. For example, the probability of missing a departure slot can be

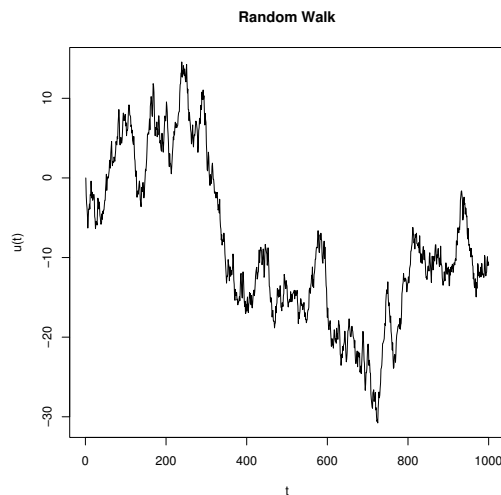


Figure 1.5: Sample trajectory of a random walk.

defined as the ratio between the number of flights with missed departure slots and the total number of flights. Note that this definition assumes that all aircraft and all conditions at take-off are considered as identical (e.g. the time-of-day has no impact on the event).

- Bayesian. Probability is defined as an individual degree of belief that an event will occur. Thus, probability is not an objective property of the outside world, but an internal state of an individual. For example, the behavior of traffic controllers during the accident at lake Constance cannot be assessed based on limiting proportions because it is a singular event. As a consequence this probability may differ between different observers.

The frequentist view has dominated probability theory during the last century. It is underlying a large part of statistical procedures, for example the logic of hypothesis tests. Often, the computational complexities of the procedures are low [Hand et al., 2001]. Bayesian probability (or more generally ‘subjective probability’) exists since the same time, but it has been primarily of theoretical interest. During the last years, due to increase in computational power, it has seen a revival. Both schools - frequentist and Bayesian - are based on the axioms of probability theory. They use the same probability calculus to derive results. It is the conclusions that may differ. On the other hand, for simple hypotheses and large data sets, the conclusions tend to be the same [Bartlett, 1975], [Hand et al., 2001].

1.3 Methodology

Before controlling uncertainty it is necessary to understand its underlying mechanisms. For example, airlines use the cancellation of flights as a strategy to avoid high departure delays [Mukherjee et al., 2005]. Or reactionary delays propagate through the whole sector network. Currently, no theory exists that explains the relationship between the predictive and the adaptive components of air-traffic management [EUROCONTROL, 2002], [EUROCONTROL, 2006]. Therefore, the approach in this thesis is to analyze past flight data to gain insight into this relationship. We consider the data as being generated by an unknown mechanism M . Input to this mechanism is a vector of variables $\mathbf{X} = \mathbf{PLN}$ representing the planned traffic. Output is a vector of variables $\mathbf{Y} = \mathbf{REAL}$ representing the real traffic. The *phenomenon* of gaps between planned and real traffic is caused by the interplay of all *uncertainty* factors in the system airspace.



Although this diagram represents the history of statistics, the principles to reach conclusions from data are still a source for controversial discussion [Chatterjee, 2003], [Lindsey, 2003], [Cox, 2006]. The naive position that empirical observation is a *basis* for scientific theories and that these are derived through an *induction principle* can still not be completely refuted but it is argued that modern epistemological theories lead to more insight in the nature of scientific discovery [Chalmers, 1982]. Also, the emergence of computing power led to ‘algorithmic approaches’ in the analysis of data [Breiman, 2001]. But these are nowadays criticized to be built on an ‘unscientific basis’ that lead to uninterpretable results [Cox, 2001], [Efron, 2001], [Saporta, 2006]. The approach in this thesis is pragmatic. It is a statistical analysis of available data.

Possible approaches

The following distinctions in analyzing data are currently made:

- (i) *exploratory vs. inferential*: In an exploratory analysis one makes statements about the data under study. In an inferential analysis one generalizes beyond the observed data and makes statements about the mechanism that generated the data.
- (ii) *prediction vs. explanation*: Prediction is the ability to generate the values of the vector \mathbf{Y} for any values of the vector \mathbf{X} . Explanation is to gain insight into the relationship $M(\mathbf{X}, \mathbf{Y})$.

- (iii) *mechanistic vs. empirical model*: Formal inferences in an analysis of data are based on the assumption that a ‘model’ has generated the observed data and not on the data itself. Several authors distinguish between ‘mechanistic’ and ‘empirical’ models [Cox, 1990], [Diggle, 1990], [Lindsey, 2003]. A mechanistic model makes assumptions about the logic of the generating mechanism. For example, traffic flow theories, e.g. [Gartner et al., 2002], [Gazis, 2002], build models of vehicle behavior since the 1950’s. They are originally formulated for highway traffic, but air traffic flow planning is sometimes inspired by them. Macroscopic fluid models [Sridhar, 2003], [Menon et al., 2004], [Bayen et al., 2006] and Wardrop equilibria and generalizations (e.g. ‘*a flow pattern is in equilibrium if no individual decision makers on the network can change it to a less costly strategy or route*’) [Altman and Wynter, 2004] are concepts to better understand fundamental properties of transportation systems with interacting users. An empirical model makes no assumption about the logic of the generating mechanism. It ‘mimics’ the relationship between input and output variables. Example are algorithmic approaches, such as neural networks and support vector machines [Breiman, 2001] or, depending on how they are justified, time-series models [Diggle, 1990]. Empirical models are typically used for prediction tasks [Cox and Wermuth, 1998], [Cox, 2001].

Position of the thesis

Given the complex structure of air-traffic management, modeling approaches can be criticized: there is currently not enough knowledge about the behavior of the actors in flow management to justify a mechanistic model. On the other hand, data-driven models with a large number of parameters are difficult to interpret. The position of this thesis is a step before modeling: we analyze past flight data in order to generate hypotheses about the behavior of the actors in ATM. This is an exploratory analysis. The results lead to a deeper understanding of the impact of uncertainties in flow planning and are useful in the construction of a realistic model of traffic flows. A recurring question in this thesis is the role of algorithms in the analysis of data.

1.4 Thesis Outline

Air-traffic management consists of a predictive component (flow planning) and an adaptive component (flow control). The aim of the predictive component is to balance airspace demand with available capacity. This takes place before take-off. Once an aircraft is in the air, the adaptive component has to guide aircraft safely to their destinations. *Uncertainties* (e.g delay from connecting flights, technical failure) lead to the phenomenon of gaps between the predictive and the adaptive component. For example in the year 2004, 17.7 % of the flights departed- and 18.5 % arrived more than 15 min behind their schedule [EUROCONTROL, 2006]. This causes safety problems and non-optimally used capacity. While the main sources of uncertainties are identified (demand uncertainties, capacity uncertainties, flow control uncertainties) the mechanisms of how they affect the components of air-traffic management remains unknown [EUROCONTROL, 2002], [Ball et al., 2005].

Main objectives

This thesis addresses the following two questions

1. are there systematic gaps between the number of planned and realized aircraft entering flight sectors?
2. how can this knowledge be used to improve current flow planning ?

If gaps occur at random, they are an unavoidable characteristic of flow planning. If not, understanding their mechanisms is a basis to control their occurrence. This is useful in tactical and pre-tactical flow planning. It leads to new constraints in the slot allocation procedure. More generally, it is the basis to close the gaps between the predictive and adaptive component in air-traffic management.

Approach

We analyze past flight data to better understand how uncertainties affect the components of flow management. We consider the data as being generated by an unknown mechanism M . Input to this mechanism is a vector of variables $\mathbf{X} = \mathbf{PLN}$ representing the planned traffic. Output is a vector of variables $\mathbf{Y} = \mathbf{REAL}$ representing the real traffic (radar data). The purpose of the analysis is to generate hypotheses about the mechanism $M(\mathbf{X}, \mathbf{Y})$ that lead to gaps between the predictive and adaptive components in air-traffic management. A permanent question is the role of algorithms in such an analysis of data.

Thesis structure

In the next section we summarize background from random vectors and statistical inference and give three examples of the analysis of multivariate data. We

then describe the data underlying our analysis. Our contributions are split into two parts: in an exploratory data analysis we analyze the phenomenon of gaps on a macroscopic level. We characterize the uncertainty about the size of the gaps, their occurrence over time and how they propagate through the sector network. One conclusion of this analysis is that gaps do occur systematically. To interpret this result we analyze the phenomenon probabilistically. In particular we analyze the impact of random disturbances on flight schedules. The two parts are independent from another and contain introductions and related works separately. The conclusions of our research are presented in the last part.

Chapter 2

Background and Data Description

A general way to analyze dependencies between random variables is to look at their joint distribution. For example the joint distribution of gaps in time-slots t and $t + 1$ is a 2×2 table containing the probabilities of all combinations of occurrences of gaps. In reality, a relationship may be simpler, for example the probability of a gap may be proportional to the probability that a gap occurred immediately before; in such cases, the joint distribution can be summarized in a compact form: $P(\text{gap}_t) = kP(\text{gap}_{t-1})$. Joint distributions — either in exhaustive or in compact form — are thus functions of outcomes of events, involving parameters. Such parameters can be estimated from observations. Based on this, the validity of the assumptions about the dependencies can be verified, for example by testing in the above case the hypothesis that $k \neq 0$. In this chapter we review elements of the analysis of multivariate data. We first summarize the main properties of random vectors. Next, we outline the role of the likelihood function in data analysis. Then we present three techniques to detect dependencies in multivariate data, illustrated by examples from the literature. Finally we describe the data underlying our analysis.

2.1 Random vectors

We introduce basic notions of vectors of discrete random variables. The reason is that our analysis is primarily concerned with counting the number of aircraft in different sectors and time-intervals. All concepts can be generalized to non-discrete random variables.

Let $\Omega \subseteq \mathbb{N}$ be a countable set of outcomes of a random experiment and $A \subseteq \Omega$ an event. Let $P : \mathcal{P}(\Omega) \mapsto [0, 1]$ be a probability on $\mathcal{P}(\Omega)$. Let $\mathbf{X} = (X_1, \dots, X_n)$ be a vector of discrete random variables $X_i : \Omega \mapsto E_i \subseteq \mathbb{N}$, $i = 1, \dots, n$.

Definition For a discrete random vector \mathbf{X} ,

$$P_{\mathbf{X}}(x_1, \dots, x_n) = P(X_1 = x_1 \cap \dots \cap X_n = x_n)$$

is the *joint probability distribution* of \mathbf{X} .

Properties:

- $\sum_{x_1, \dots, x_n} P_{\mathbf{X}}(x_1, \dots, x_n) = 1$
- when the domains E_i are finite, the distribution is represented by a table.

Example: First-order Markov Chain. The table below shows the joint probability distribution of the two random variables X_{t-1}, X_t , where $X_t = 1$ is the event ‘a gap occurs in time-slot t ’. It contains 4 parameters, one for each combination of the outcome of the events ‘gap occurs in time slot t ’ and $t+1$. In the general case, all cell probabilities are unknown. Only the constraint that they sum to unity eliminates one parameter.

	X_t	0	1
X_{t-1}		0	1 - (p+kp)
		p	kp

To come back to the example in the introduction, the distribution contains a parameter, k , translating the assumption that the probability of a gap is proportional to the previous occurrence probability. Another assumption in this example is that the event ‘no gap - no gap’ never occurs. This is unrealistic but illustrates the further discussion.

Definition Let \mathbf{X} be a discrete random vector. The probability distribution of the i -th component

$$P_{X_i}(x_i) = \sum_{\{x_1, \dots, x_n\} \setminus \{x_i\}} P_{\mathbf{X}}(x_1, \dots, x_n)$$

is the i -th *marginal distribution* of \mathbf{X} .

In the example above $P_{X_t}(x_t = 0) = p$ and $P_{X_t}(x_t = 1) = 1 - p$.

Definition Let X, Y be two discrete random variables.

$$P_{Y|X}(y | x) := P(Y = y | X = x) = \frac{P_{XY}(x, y)}{P_X(x)}, \quad \forall x : P_X(x) > 0$$

is the *conditional distribution* of Y given X , and it is undefined if $P_X(x) = 0$.

In the example above $P(X_t = 0 | X_{t-1} = 0) = 0$ and $P(X_t = 1 | X_{t-1} = 0) = 1$. Note that the marginal and the conditional distributions differ substantially.

Independence

The intuition behind independence between random variables is that the distribution of one variable is unaffected by knowledge of the values of other variables. We will define independence between two variables and its generalization to several variables.

Definition Two random variables X, Y are *independent* if

$$P_{X,Y}(x, y) = P_X(x)P_Y(y), \quad \forall x, y$$

Example: Poisson process. In a Poisson process, the number of arrivals in distinct intervals are independent Poisson variables. Let $N(a_i, b_i)$ be the number of arrivals in the interval $(a_i, b_i] \subset \mathbb{R}$ with $a_i < b_i \leq a_{i+1}$. Then

$$\begin{aligned} P(N(a_i, b_i) = n_i, i = 1, \dots, k) &= \prod_{i=1}^k P(N(a_i, b_i) = n_i) \\ &= \prod_{i=1}^k \frac{\lambda(b_i - a_i)^{n_i}}{n_i!} e^{-\lambda(b_i - a_i)}, \quad \forall k \end{aligned}$$

Definition Two random variables X, Y are *conditionally independent* given a random vector $Z = (Z_1, \dots, Z_n)$ when

$$P(X | Y, Z) = P(X | Z)$$

Example: First-order Markov Process. In a first order Markov process, the state of the process at time X_{t+1} is independent of the past X_{t-2}, \dots, X_1 , given the present state X_t :

$$P(X_t | X_{t-1}, X_{t-2}, \dots, X_1) = P(X_t | X_{t-1})$$

The joint distribution becomes

$$P_{\mathbf{X}}(x_1, \dots, x_n) = P_{X_1}(x_1) \prod_{i=2}^n P(X_i | X_{i-1})$$

Correlation

Expressing dependencies between random variables by their joint distribution is not always practical: there are too many parameters to determine and to interpret. A special case of dependency between two random variables is linear correlation. It expresses the idea that a value above average of one variable is associated with a value above average of the other variable. Linear correlation is often used as an approximate description of the real relationship between two variables [Cox and Wermuth, 1998]. For a vector $\mathbf{X} = (X_1, \dots, X_n)$ of random variables, the correlation is a $n \times n$ matrix of pairwise linear correlations.

Definition The *mean vector* and *covariance matrix* of a random vector $\mathbf{X} = (X_1, \dots, X_n)$ are

$$\mathbf{E}(\mathbf{X}) = \boldsymbol{\mu}_x = \begin{bmatrix} \mathbf{E}(X_1) \\ \mathbf{E}(X_2) \\ \vdots \\ \mathbf{E}(X_n) \end{bmatrix}$$

and

$$\boldsymbol{\Sigma}_X = \mathbf{E}[(\mathbf{X} - \boldsymbol{\mu}_x)(\mathbf{X} - \boldsymbol{\mu}_x)'] = \begin{bmatrix} \sigma_1^2 & \text{cov}(X_1, X_2) & \dots & \text{cov}(X_1, X_n) \\ \vdots & \vdots & \dots & \vdots \\ \dots & \dots & \dots & \dots \\ \dots & \dots & \dots & \sigma_n^2 \end{bmatrix}$$

The *correlation matrix* is defined by

$$\boldsymbol{\rho}_X = \mathbf{D}^{-1/2} \boldsymbol{\Sigma}_X \mathbf{D}^{-1/2} = [\rho_{ij}]$$

for $i, j = 1, 2, \dots, m$ where \mathbf{D} is the diagonal matrix in which the i th diagonal element is the variance of the i th component:

$$\mathbf{D} = \text{diag}[\sigma_1^2, \sigma_2^2, \dots, \sigma_n^2]$$

2.2 Likelihood

Based on a probabilistic model, statistical inference allows to quantify uncertainty about the existence of structure in observations. For example one can assume a relationship between two variables X, Y . An estimation of the strength of the relationship may result in a value near 0. Based on a hypothesis test, one may reject the hypothesis that the relationship exists in reality.

Likelihood function

Given a probabilistic model with parameters $\theta \in \mathbb{R}^p$ and observations $D = (y_1, \dots, y_n)$ the likelihood

$$L_\theta(D) = P_{\mathbf{X}}(y_1, \dots, y_n \mid \theta) \quad (2.1)$$

is the joint probability of the observations given the parameters θ . The value $\hat{\theta}$ which maximizes 2.1 is called the maximum likelihood estimate. Knowledge of independence or conditional independence between the observations can be used to factorize this joint distribution into a product form.

Example: Poisson process (continuation). Let $D = (y_1, \dots, y_n)$, where y_i is the number of arrivals in unit-time interval i , be observations of a realization of a Poisson process with rate λ . The likelihood of the observations is:

$$\begin{aligned} L_\lambda(D) &= \prod_{i=1}^n P(N(i, i+1) = y_i) \\ &= \prod_{i=1}^n \frac{\lambda^{y_i}}{y_i!} e^{-\lambda} \end{aligned}$$

Taking the logarithm on both sides leads to

$$l_\lambda(D) = \sum_{i=1}^n y_i \log(\lambda) - \lambda - \log(y_i!)$$

Solving $\frac{\partial l}{\partial \lambda} = 0$ gives $\hat{\lambda} = \sum n_i/n$, the sample mean. Note that this calculation is a special case of $\lambda_i = f(X_i)$, the Poisson regression model, that we will use in chapter 3.3.

The likelihood is a central concept in statistical inference. For example in hypothesis tests, the assumed model (the null hypothesis) is rejected, if the probability of the observed data is less than the significance level. There is also an approach to base inference uniquely on the likelihood ("*a model that makes the observed data more probable is more likely to have generated the data*") [Edwards, 1972], [Pawitan, 2001], [Lindsey, 2003]. This direct likelihood approach is criticized to be of predictive value rather than of explanatory value and an open question in statistical inference is which additional arguments are

necessary to derive useful information from the likelihood [Cox, 2006]. As seen in the example above, likelihood is also used in estimation of parameters, where the ‘best’ parameter of a model is defined as the one that maximizes the likelihood. This leads to consistent estimators. But they can be biased and inappropriate for small sample sizes [Saporta, 2006].

Parameter estimation

When no closed-form solution for the maximum of 2.1 exists, numerical algorithms can be used. A general form of the optimization problem is

$$\begin{aligned} \min \quad & f_0(x) \\ \text{s.t.} \quad & f_i(x) \leq 0, \quad i = 1, \dots, m \cup \{\emptyset\} \end{aligned} \quad (2.2)$$

where $x = (x_1, \dots, x_n) \in \mathbb{R}^n$ are decision variables, $f_0 : \mathbb{R}^n \mapsto \mathbb{R}$ is the objective function and $f_i : \mathbb{R}^n \mapsto \mathbb{R}$ are (optional) constraints. For example, f_0 corresponds to the negative likelihood function, x to the model parameters, and the f_i to constraints on model parameters, such as non-negativity.

The following problem classes are known [Boyd and Vandenberghe, 2004]

Linear and convex problems

(the f_i are convex functions)

Optimal solutions to problem 2.2 are obtained by

- gradient descent, Newton (for unconstrained problems).
- Simplex algorithm, interior point methods.

The complexity of linear optimization problems is polynomial in n, m . For some unconstrained and convex problems, polynomial algorithms exist.

Non-linear problems

(the f_i are non-convex functions)

The worst case complexity of problem 2.2 grows exponentially with problem size n, m . One reason is that the optimal solutions no more lie on the edges of the feasible region, as is the case with linear problems. Two general approaches are

- local optimization (meta-heuristics) [Aarts and Lenstra, 1997]. A local optimum is found.
- global optimization [Liberti and Maculan, 2006]. The global optimum is found. These problems are more interesting from a theoretical point of view. Solutions are restricted to problems with a small number of variables.

2.3 Examples from Multivariate Data Analysis

We give three examples from the analysis of multivariate data. We distinguish asymmetric relationships, where a variable X has impact on another variable Y from symmetric relationships, where two variables X, Y mutually depend on themselves.

Open-loop systems

For an asymmetric relationship between two processes X_t, Y_t , a family of models is

$$Y_t = \sum_{k=-\infty}^{\infty} \phi_k X_{t-k} + \epsilon_t \quad (2.3)$$

where ϵ_t is some stochastic error. Equation 2.3 is sometimes called ‘transfer function model’ or ‘open loop linear system’. Techniques to identify a linear transfer function between stationary processes include cross-correlation and cross-spectrum. To eliminate spurious correlations that are caused by serial correlation in the individual processes, different forms of pre-whitening are proposed in literature [Kendall, 1989], [Diggle, 1990]. A whitening procedure has an impact on the interpretation of the parameters [Diggle, 1990]. Inclusion of several processes on the right side $X_{jt}, 1 \leq j \leq n$ is in principle possible but raises problems with the interpretation of parameters.

For example [Majumdar et al., 2005] analyze the factors that affect controllers workload in a sector. Examples of such factors are the number of aircraft in cruise profile or the number of entries in neighboring sectors. They believe that these factors have the same effect in every sector, but that different sectors have different characteristics due to local, unobserved events (e.g. working environment). In essence, their model is an open-loop system taking into account possible differences between sectors. They identify a number of significant factors with a potential impact on workload. Their validation is mainly based on predictive accuracy of the model, so they can only conclude that they found factors that are useful to predict controllers workload. In an analysis of data with similar characteristics (daily repeating patterns, dependency on external events) [Giot, 2001] model their process initially as an auto-regressive time series. Then, they analyze the impact from external covariates and find significant changes in the auto-regressive components. Thus the interpretation of the initial model is revised.

Multivariate time-series

A family of models for symmetric relationships between processes is based on the following idea:

$$\begin{aligned} X_t &= \phi_{11}X_{t-1} + \phi_{12}Y_{t-1} \\ Y_t &= \phi_{21}Y_{t-1} + \phi_{22}X_{t-1} \end{aligned} \quad (2.4)$$

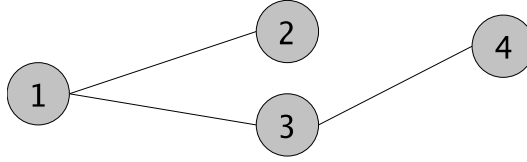


Figure 2.1: Example for an undirected graphical model. X_1 is conditionally independent of X_4 given X_2 and X_3 . In normal theory, the partial correlation $\rho_{1,4|2,3}$ would equal 0 under such conditions.

They mutually depend on themselves. The standard stochastic model includes additive noise $\epsilon_{t_i}, i \in \{x, y\}$ which has zero mean, is uncorrelated over time but may be correlated between the components ϵ_{t_x} and ϵ_{t_y} (There are other formalisms which express this instantaneous dependency explicitly, discussed in [Greene, 2002]). In matrix notation, such systems can be written as $\mathbf{Y}_t = \sum_{j=1}^{\infty} \phi_j \mathbf{Y}_{t-j} + \epsilon_t$ where \mathbf{Y}_{t-i} are k -dimensional vectors and ϕ_i are $k \times k$ matrices of parameters to be estimated. Model families of this type are discussed in time-series literature. The above corresponds to vector-autoregressive processes (VAR). Vector moving average (VMA) and vector autoregressive moving average (VARMA) models are defined similarly e.g. [Box and F.Jenkins, 1970], [Kendall, 1989]. Identification techniques include correlation - and partial correlation matrix functions for stationary processes.

Graphical models

Dependency structures based on conditional independence can be described by graphs $G = (V, E)$, where a random variable X_i is associated to each vertex $i \in V$. The absence of an edge between two vertices i, j means that the variables X_i, X_j are conditionally independent given the others, denoted by $X_i \perp X_j | Z$. Graphical models are discussed from several perspectives, e.g. [Edwards, 1972], [Whittaker, 1990] for statistical - or [Pearl, 1988] for probabilistic questions. Techniques to identify graphical dependency structures in data include partial correlation and partial coherence analysis [Brillinger, 1996], [Cox and Wermuth, 1998]. For example, when the variables are jointly normally distributed, conditional independence between X and Y given Z is equivalent to $\rho_{X,Y|Z} = 0$, the partial correlation coefficient [Whittaker, 1990], [Lauritzen, 1996]. For example, Figure 2.1 shows an undirected graphical model with four nodes. $X_1 \perp X_4 | \{X_2, X_3\}$ is equivalent to $\rho_{1,4|2,3} = 0$. Similar results exist for directed graphs (representing asymmetric relationships) and for discrete variables [Edwards, 1972], [Cox and Wermuth, 1998].

For example, [Brillinger and Villa, 1997] analyze dependencies in a system of Point processes. A node in their graph corresponds to a stationary Point process. Dependency between processes are measured via coherency and par-

tial coherency function. They infer that dependency between two processes exists, even after removing the linear impact from a third one. However, they speculate that some of the significant dependencies are due to a time trend (non-stationarity).

2.4 Data Description

We analyze data from two sources. The first source is the flow planning process, creating daily flight schedules that satisfy the sector capacity constraints. The second source is radar data which updates the flight schedules with the real flown trajectories. While the first source is deterministic (it is the outcome of the slot allocation algorithm), the radar data contains implicitly the impact of all uncertainty factors on the flights. Eurocontrol stores both data types in a centralized data base which is updated daily. In this section we explain general characteristics of the data - its format, its temporal- and geographical dimension and its quality -, necessary for data selection and pre-processing.

Format and type

Flight data is either trajectory-based or sector-based. In trajectory based data, sequences (S_i, t_i) of sectors and entry-times exist for every aircraft. In sector based data, the number of aircraft entering a sector in a given time interval exists for every sector. Both data types are numerical; the trajectory-based data are real numbers and the sector-based are natural numbers.

Trajectory profiles

A flight plan has the form

$$(S_1, t_1), \dots, (S_n, t_n)$$

where S_i are sectors and t_i are the entry times in the sectors. S_1 is the departure airport and t_1 is the time of the runway access.

For every flight, three flight profiles are available

1. Filed profile. This is the initial flight plan that is submitted by the airlines to the control center.
2. Regulated profile. This is the profile with possibly delayed departure time $t'_1 \geq t_1$.
3. Current profile. This is the real flown profile. It is based on radar information. A field (S_i, t_i) of the regulated profile is updated if its difference with the real position of the aircraft is greater than 200 NM or longer than 5 minutes.

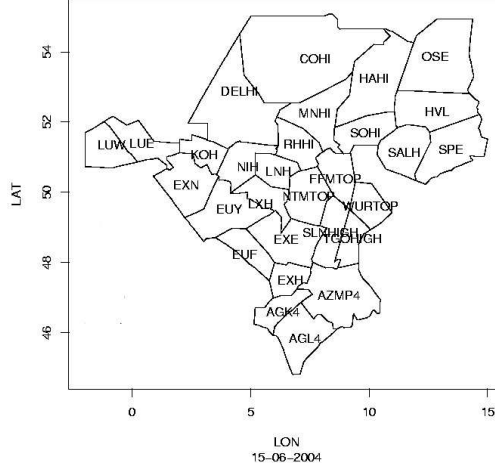


Figure 2.2: Central European Upper Airspace.

Sector profiles

For a sector S , the number of flights that enter it in a time interval $t = (t_s, t_e]$ is called the sector profile. It is obtained from the flight profiles by aggregation

$$X_i^S = \sum_{i=1}^N \sum_{j=1}^{i_n} \mathcal{I}_S(S_{i_j}) \mathcal{I}_T(t_{i_j})$$

where N is the number of flights, $\mathcal{I}_S(S_i) = 1$ iff $S_i = S$ and $\mathcal{I}_T(t_i) = 1$ iff $t_i \in t$. As with the three flight profiles, three sector profiles (filed profile, regulated profile and current profile) exist for every sector.

Period

Air-traffic demand is growing yearly. The top part of Figure 2.3 shows the numbers of million flights per year since 1990. For example in 2005, 9.2 million flights were controlled in Europe. This is an increase of 3.9. % relative to the previous year. Traffic growth is forecast to continue at an annual rate of 3 % to 4 %. The monthly traffic demand can be seen in the bottom part of Figure 2.3. From January until May, traffic demand is increasing. The summer months (June-September) are stable, followed by a decrease until December. The daily averages fall between 22.000 in winter- and 28.000 flights in summer. Finally, two distinct demand types exist: week-day (Mon-Thu) and week-end (Fri-Sun) [EUROCONTROL, 2006].

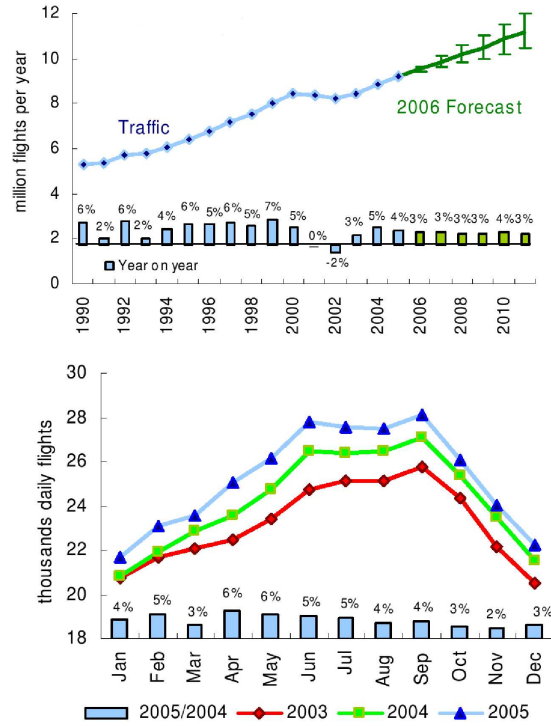


Figure 2.3: Traffic Evolution. Yearly trend (top). Monthly seasons (bottom). Source: EUROCONTROL

We select data of 75 week days (Mon-Thu) in the summer period 13.5.-29.9.2004. We assume similar traffic conditions (number of flights, network topology, controllers) for each of these days.

Geographic area

Figure 2.2 shows the geographical area of our study. The area covers the upper airspace between London, Zurich and Berlin. The control of this area is shared between 31 elementary sectors belonging to 9 flow centers. The average traversal time of a sector in this region is 7 minutes. The reason to analyze sectors in this area is that the area has the highest risk of congestion.

Quality

As a consequence of the huge amount of data (> 20000 flight plans per day) and the partly manual processing, errors in the flight plans are unavoidable. For example flight plans with ‘leaks’ in the route sequences exist or stored flight

plans may be inaccurate due to last-minute modifications. There is a whole service, the Initial Flight Plan Processing Unit (IFPU) that is responsible for the quality of flight plan data. However, about 5 % of the total flight plans have to be considered inaccurate. We use the data extraction functionality of the certified COSAAC tool (Common Simulator to Assess ATFM Concepts [EUROCONTROL, 2004]) to further minimize the amount of inconsistent data, assuming that controllers discern obvious inaccuracies in advance, as well.

Chapter 3

Results of Exploratory Analysis

There are many reasons why aircraft deviate from their flight plans: pilots wait for delayed connecting flights or take shortcuts to recover departure delays. Air-traffic controllers solve conflicts by speed- and route adjustments of aircraft. Finally, weather conditions force pilots to avoid certain sectors or have an impact on the speed of aircraft. Deviations from flight plans lead to gaps between the number of planned and realized entries at sectors. This leads to safety problems and sub-optimally used capacity.

In this chapter we analyze the following questions:

- do gaps between the number of planned and realized aircraft occur systematically?
- or are they compensated by the behavior of traffic controllers and pilots?

If they occur at random, they are an unavoidable characteristic of the flow planning system. If not, understanding their mechanisms can help to control the occurrence of gaps.

Description of gaps between planned and realized traffic

The approach is to analyze past flight data to *describe* the gaps: their occurrence, their magnitude and their propagation through the sector network. We explore and summarize regularities in the data. Such an activity has several names: exploratory data analysis [Tukey, 1977], *analyse des données* [Saporta, 2006] or data mining [Hand et al., 2001]; the main characteristic is that we do not make assumptions about the phenomenon.

Methodology

For a single sector we consider $\{y_t\}, t = 0, 1, 2, \dots$ as a sequence of observations (e.g. the number of aircraft) in time slot t . Two standard approaches to analyze such sequences are time-series analysis [Kendall, 1989], [Diggle, 1990], and signal processing [Mallat, 2000]. In a first step, both try to identify patterns, for example periodicity (e.g. daily repetitions), time-trends (e.g. yearly increase) or edges (sharp increases in gradient). The main techniques are smoothing, correlation- and frequency analysis.

For m sectors, observations in slot t are represented as m -dimensional vectors $\{\mathbf{y}_t\}, t = 0, 1, 2, \dots$. We are interested in the question 'if there is a gap in sector S at time t , how does it affect the other sectors at time $t + k$?'. Such situations can be seen as open-loop or multivariate systems. The identification techniques are mostly generalizations of the univariate case: correlation matrices and cross-spectral densities.

Descriptive data analysis is subjective and one should always ask why a given series shows a particular pattern. For example a linear trend on a small time-scale can appear as part of an oscillation effect when the time horizon is widened [Kendall, 1989]. [Diggle, 1990] identifies other limitations of pure data-driven approaches to time series analysis.

Formalization

We analyze the relationship between the two components 'planned traffic' and 'realized traffic'. More formally, we analyze the relationship between the two processes

$$\{\mathbf{PLN}_t : t \in \mathbb{N}\} \text{ (deterministic)} \quad (3.1)$$

$$\{\mathbf{REAL}_t : t \in \mathbb{N}\} \text{ (stochastic)} \quad (3.2)$$

The first process (3.1) is the process of flow planning, mapping demand on available departure slots. This process has been described in the introduction; it is based on flight plans and sector capacities. The second one (3.2) is stochastic, mapping the outcome of a planning onto the number of real arrivals.

Given N observations of planned and realized traffic in p sectors

$$D = \{(\mathbf{real}_i, \mathbf{pln}_i)\}_{i=1}^N, \mathbf{real}_i, \mathbf{pln}_i \in \mathbb{N}^m$$

we answer two questions: (i) do gaps between planned and realized traffic occur systematically? and (ii) how do the gaps propagate through the system?

Related work

[Wanke et al., 2003] and [Wanke et al., 2005] analyze the aggregate effect of uncertainties in sector demand in the U.S. airspace. They identify binomial- and

Poisson distributed counts of aircraft entering flight sectors. They also identify major factors with an influence on these distributions. They conclude that uncertainty is increasing with a higher prediction horizon. This can be partially explained by ‘pop-up’ flights, not yet having submitted their flight plans.

[Robelin et al., 2006] analyze radar data to identify real traffic flows in the U.S. airspace. They define a flow as a cluster of aircraft with similar trajectory properties. A trajectory is a high-dimensional vector of geographical components. They use k-means, principal component analysis and syntactic matching to identify the clusters. Even after enhancing the data set with additional features (e.g. aircraft type), they conclude that none of the algorithms provides satisfactory results for practical purposes.

[Hansen and Wei, 1999] analyze empirically the daily variation in flight delays. They build a non-linear regression model relating average flight time with external variables (e.g. demand, weather, origin) and interactions between them. Their aggregate approach allows them to assume independence between daily observations. They conclude that a capacity expansion that had taken place in the past lead to an average decrease of delays, particularly under low visibility conditions. However, they relative their observation by pointing out that the capacity expansion may have caused an increase in demand, causing higher delays again.

Plan of the chapter

The analysis consists of three parts parts, a validation and an interpretation.

First we propose three definitions of gaps between planned and realized sector entries. Each one offers insight in the characteristics of the phenomenon. We describe their main properties and fit parametric distributions. Then we analyze gaps in a single sector. We show that their occurrence is time-invariant and that their relationship with traffic density is non-linear. In the third part we analyze how gaps propagate through the sector network. We estimate correlations between gaps in different sectors and different times and conclude that no unexpected correlations are identified. We validate the results on different time-scales and on randomly chosen sectors. Finally, we interpret the results and give the main conclusions.

3.1 Summary of Results

Uncertainty of gaps

We give three different definitions of gaps between the number of planned and realized aircraft in a flight sector. The marginal distributions of direct definitions of gaps have higher probabilities in the tails and close to the center than normal and log-normal distributions. Defining gaps as a function of planned traffic leads to Poisson distributions. These results characterize the uncertainty about the size of gaps.

Systematic gaps between planned and realized

For low traffic densities, systematically more aircraft than planned arrive. For high traffic densities, the inverse is true. This relationship can equally well be characterized by a logarithmic, square-root or reciprocal function of planned traffic. We conclude that systematic gaps between the number of planned and realized traffic exist.

Propagation of gaps

We analyze how gaps between planned and realized traffic propagate through the network of flight sectors. We first develop bounds of the variability of coefficients of the sample correlation matrix function as a function of the sample size and the dimension of the problem. Applied to the most congested part of the network shows that significant correlations appear on two levels: (i) locally, that is between a sector and its direct neighbors and (ii) globally on ‘traffic highways’, that is between sectors that are connected through a flight route with high traffic densities. From those pairs of sectors that are correlated, 84 % have exactly one significant coefficient and there are never more than 4 significant coefficients. Moreover, all correlations are positive and their time-lags correspond to the average traversal times. No unexpected correlations have been found. This is evidence that no systematic re-routing is initiated by air-traffic controllers.

3.2 Uncertainty of Gaps

Gaps are differences between the number of planned and realized entries into a flight sector. Three possible definitions are

$$GAP_t = \begin{cases} REAL_t - PLN_t & \text{absolute definition} \\ REAL_t/PLN_t & \text{relative definition} \\ f(REAL_t, PLN_t, \mathbf{X}) & \text{functional definition} \end{cases}$$

All three definitions give insight in the phenomenon. For example absolute and relative gaps describe directly how the phenomenon appears to an observer. The functional definition models the joint distribution of $REAL$ and PLN . \mathbf{X} is a vector describing the environment in which the variables are observed, for example the time of the day. It gives insight into how gaps are generated by the flow planning component.

In this section we describe the marginal distributions P_{GAP_t} of all three definitions. Unlike conditional distributions $P(X_t | X_{t-1}, X_{t-2}, \dots)$, marginal distributions cannot completely specify a process. Moreover, observations x_1, x_2, \dots, x_n of a stochastic process are usually not independent. Sampling its marginal distributions can be biased. On the other hand, marginal distributions summarize the global variation of the process. Sometimes they also provide insight in its dependency structure [Baccelli, 2002], [Cappé et al., 2002]. When not stated otherwise, we report results from sampling marginal distributions of a single long realization of the stationary process GAP_t .

The upper panel of Figure 3.1 shows a time plot of 4 successive week-days of traffic. The round circles on the $y = 0$ line mark the beginning of a new day. The number of arrivals is counted in 15 minutes time intervals. One day consists of 96 intervals. The range of the variables is $[0,15]$. The dotted line is the planned traffic. The bold line is the realized traffic, shifted by 10. Their shapes are similar. Daily repeating patterns are visible. A typical daily pattern can be described as ‘few traffic in the night, irregular pattern during the day (7-19h)’. In some sectors, peaks at noon and in the afternoon arise, but this is not the general case [Guerreau, 2000]. For example, some sectors have peak hours due to the arrival of over-Atlantic flights, other sectors lie close to airport and have constant densities over the day. In the middle panel the absolute definition of gaps $PLN_t - REAL_t$ is plotted over time. It fluctuates around 0. The variance looks constant during the day (7-19h) and during the night. In the lowest panel, the relative definition of gaps $GAP_t = REAL_t/PLN_t$ is plotted. Apart from two high peaks in the first day, the series fluctuates around the value 1. Here the variance during the day (7-19h) appears to be smaller than during the night.

Figure 3.2 shows the sample autocorrelation function of the series $GAP_t = REAL_t - PLN_t$ (top) and $GAP_t = REAL_t/PLN_t$ (bottom)

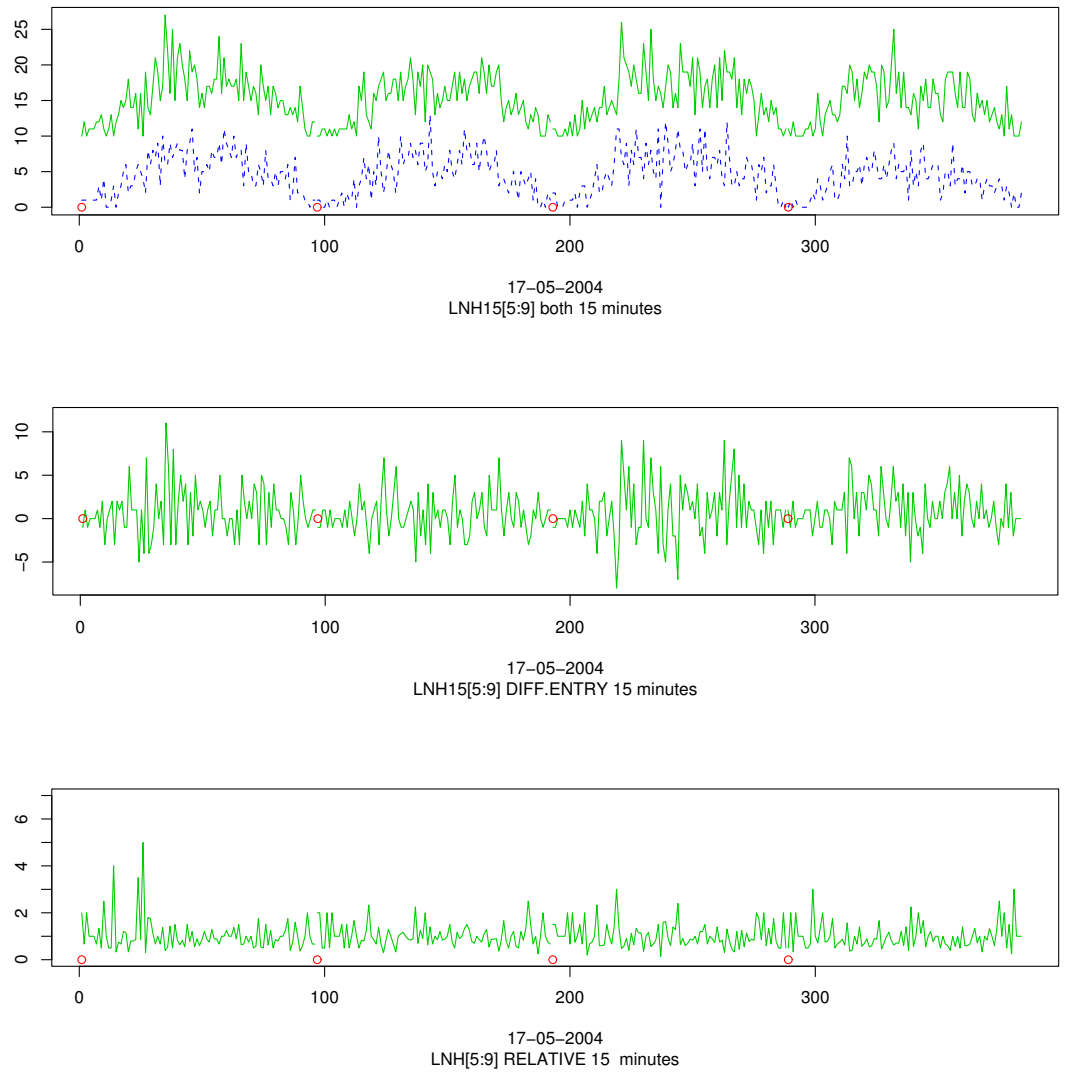


Figure 3.1: Time plots of 4 successive week-days of traffic. Top: realized traffic REAL (dotted) and planned traffic PLN, shifted by 10 (bold). Middle: REAL-PLN. Bottom: REAL/PLN.

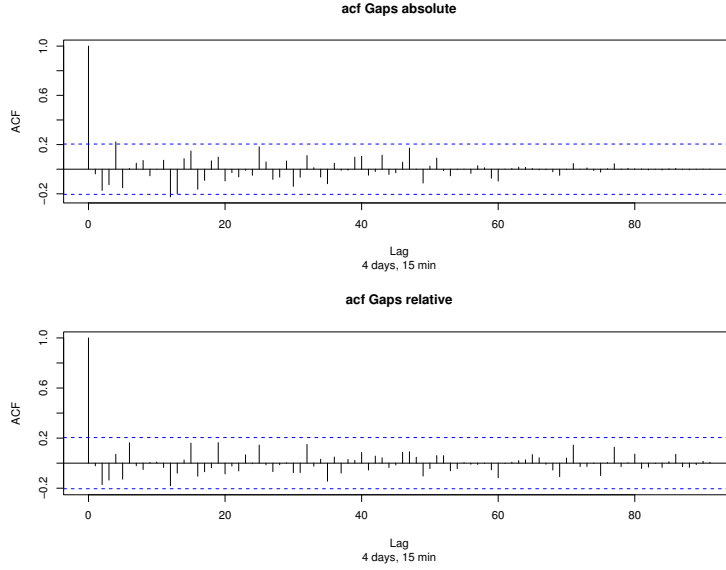


Figure 3.2: Sample autocorrelation functions for gaps of 4 successive days ($n=384$). Top: absolute gaps $GAP_t = REAL_t - PLN_t$. Bottom: relative gaps $GAP_t = REAL_t/PLN_t$.

$$\hat{\rho}(k) = \frac{\sum_{i=1}^{N-k} (x_i - \hat{\mu})(x_{i+k} - \hat{\mu})}{\sum_{i=1}^N (x_i - \hat{\mu})^2}, \quad 0 \leq k \leq 96$$

of one day. $\hat{\mu} = \frac{1}{N} \sum_{i=1}^N x_i$. The horizontal lines delimit the 95 % confidence interval for the autocorrelation of an i.i.d. process. No meaningful significant coefficients appear in both plots.

Absolute

Figure 3.3 shows the histogram of the marginal distribution of absolute gaps $GAP_t = REAL_t - PLN_t$ during the day (7-19h). It is a symmetric distribution. Its mean and standard deviation are 1.2 and 3.2 respectively. Superposed is a normal distribution with density

$$pr(x) = \frac{1}{\sigma\sqrt{2\pi}} e^{-\frac{(x-\mu)^2}{2\sigma^2}}$$

Except from a peak at $GAP_t = 0$ the distribution fits the data accurately. Table 3.1 shows descriptive statistics for five randomly selected sectors. They all have first four moments that characterize a Gaussian distribution: mean ~ 0 , standard deviation ~ 3 , skewness ~ 0 and kurtosis ~ 3 . System-wide, the means

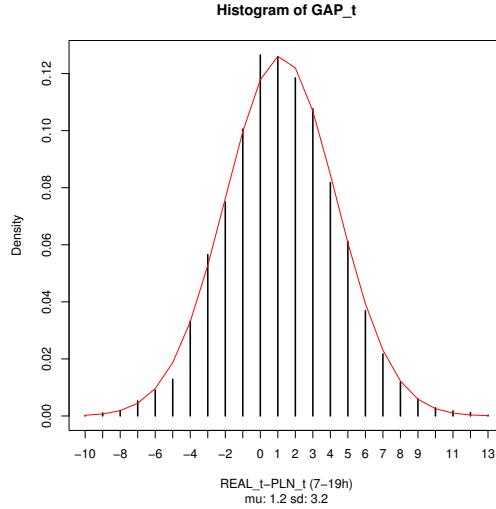


Figure 3.3: Histogram of absolute gaps $GAP_t = REAL_t - PLN_t$ (7-19h).

of all 31 distributions lie in the range $[-1.3, 1.0]$. Their standard deviations lie in $[1.9, 3.7]$, skewness in $[-0.1, 0.1]$ and kurtosis in $[2.9, 3.4]$ (last row). Figure 3.4 shows the q-q plot where the distributions of all 31 sectors are superposed. The data has been standardized, so the diagonal is the 45-degree line. The plot indicates that the tails of the sample distributions have higher probability than those of a Gaussian distribution.

Relative

The left part of Figure 3.5 shows the histogram of the marginal distribution of $GAP_t = REAL_t / PLN_t$ during the day (7-19h). It is antisymmetric to the right with mean=1.3, sd=0.69 and skewness=3.1. Superposed is a log-normal distribution with density

$$pr(x) = \frac{e^{-(\ln x - \mu)^2 / (2\sigma^2)}}{\sigma x \sqrt{2\pi}}$$

Its density around the center is too small. One can summarize the distribution as follows:

$\leq -50\%$	-25%	$\pm 10\%$	$+ 25\%$	$\geq 50\%$
0.04	0.25	0.17	0.3	0.24

In 4 % of the cases, $REAL_t$ is less than 50 % of PLN_t . In 25 % of the cases, it is around 25 % of it. Situations in which $REAL_t$ is $\pm 10\%$ of PLN_t occurs

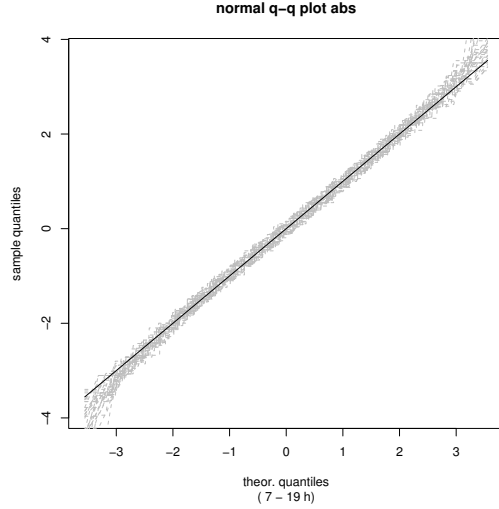


Figure 3.4: q-q plots for absolute gaps of 31 sectors (7-19h).

Sector	N	μ	sd	skew	kurt	min	max
EUJ	3675	0.08	3	0.01	3.2	-12	11
CLEU	3675	-0.23	2.2	-0.01	3.2	-9	8
KOH	3675	0.89	3.2	0.02	3	-10	12
HVL	3675	0.19	3	0.00	3.1	-15	11
EUJ	3675	0.27	3.2	0.04	3.4	-14	13
all		[-1.3,1.0]	[1.9,3.7]	[-0.1, 0.1]	[2.9, 3.4]	[-18,-9]	[8,15]

Table 3.1: Marginal distribution of absolute gaps $GAP_t = REAL_t - PLN_t$ (7-19h). 5 randomly selected sectors. Last row: all 31 sectors.

in 17 % of the cases. In 30 % of the cases, $REAL_t$ is 25 % higher than PLN_t . The remaining cases account for 24 % of the distribution.

The right part shows their logarithm $GAP_t = \log(REAL_t/PLN_t)$. This distribution is unsymmetrical, as well. It has mean=0.16, sd=0.52 and skewness=0.25. However, a Gaussian distribution is superposed. It fits the data accurately, even if its density around the center is too small. Table 3.2 shows descriptive statistics for this representation of relative gaps. Half of them are negatively skewed. All of them have a kurtosis higher than a Gaussian distribution. In all 31 sectors, skewness lies in the interval $[-0.24, 0.46]$ and kurtosis in $[3.9, 6.2]$ (last row). The q-q plot for all 31 sectors can be seen in Figure 3.6. Two features appear: the tails contain more density than Gaussian distributions and

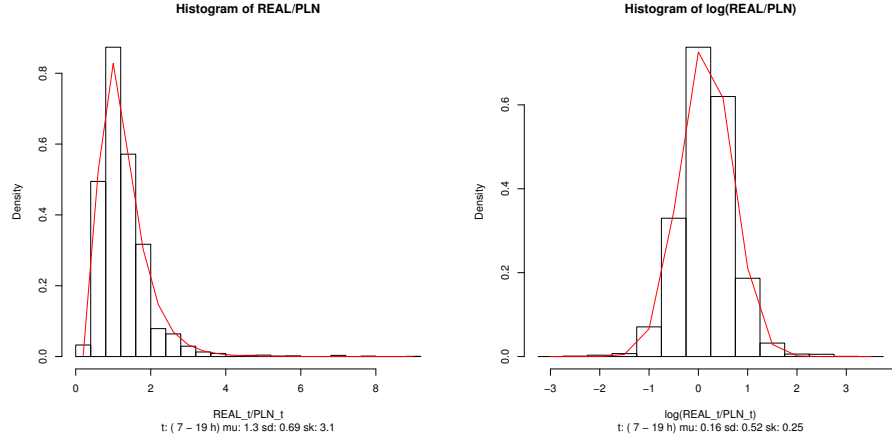


Figure 3.5: Histograms of relative gaps $GAP_t = REAL_t/PLN_t$ (left) and of their logarithm (right).

Sector	N	μ	sd	skew	kurt	min	max
SLNHIGH	3675	0.02	0.48	-0.02	4.8	-2.4	2.4
LNH	3675	-0.17	0.5	-0.28	4.5	-2.9	2.2
HAHI	3675	-0.10	0.48	-0.21	5.4	-2.8	2.8
EUY	3675	0.038	0.46	0.10	4.6	-2.6	2.4
AGL4	3675	0.15	0.61	0.46	4.9	-2.4	3.1
all		[-0.17, 0.16]	[0.39,0.66]	[-0.24,0.46]	[3.9,6.2]	[-3.0,-1.6]	[1.8,3.2]

Table 3.2: Marginal distribution of relative gaps $GAP_t = \log(REAL_t - PLN_t)$ (7-19h) on 5 randomly selected sectors. Last row: all 31 sectors.

the density around the center is higher than for Gaussian distributions. Both features explain the high kurtosis.

Functional

Figure 3.7 shows two histograms of the variables $REAL_t$. On the left, it is conditioned on the time-of-day t : $P(REAL_t|t)$. In the example, the time-slot corresponds to $16h - 16h15$. This corresponds to sampling the distribution from different daily realizations. The values can thus be assumed to be independent from each other. On the right, it is conditioned on the planned traffic PLN_t : $P(REAL_t|PLN_t)$. In the example $PLN_t = 4$. Both distributions are right skewed. The variables are positive (including 0) and discrete. Superposed are Poisson (green) and binomial distributions (red).

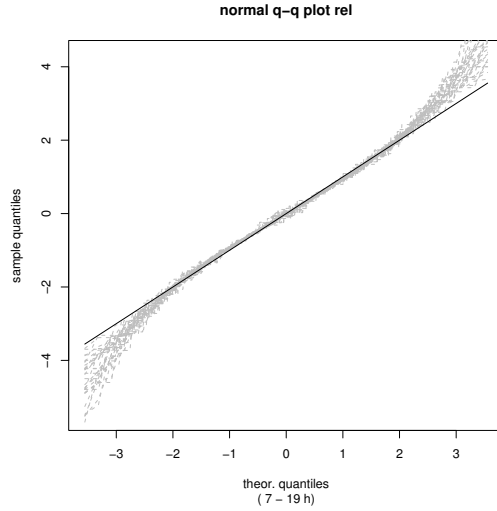


Figure 3.6: q-q plots for relative gaps of 31 sectors (7-19h).

The Poisson distribution has mass

$$P_{\lambda}(Y = k) = \frac{\lambda^k e^{-\lambda}}{k!}$$

with parameter λ . Its first two moments are

$$\begin{aligned} \mathbf{E}(Y) &= \lambda \\ \mathbf{V}(Y) &= \lambda \end{aligned}$$

The binomial distribution has mass

$$P_{n,p}(Y = k) = \binom{n}{k} p^k (1-p)^{(n-k)}$$

with mean and variance

$$\begin{aligned} \mathbf{E}(Y) &= np \\ \mathbf{V}(Y) &= np(1-p) \end{aligned}$$

where p is the probability of occurrence, k is the number of occurrences and n is the number of trials. Given N observations (y_1, \dots, y_N) , the maximum likelihood estimator for p is:

$$\hat{p} = \frac{\sum_{i=1}^N y_i}{Nn}$$

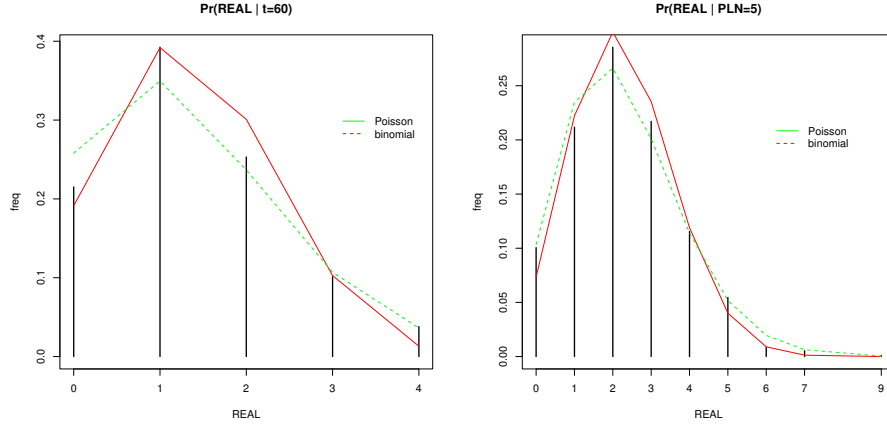


Figure 3.7: Number of real arrivals ($REAL_t$) conditioned on time of day (left) and on number of planned entries (PLN_t) (right).

Distribution	Cond.	χ^2
Poisson	t	75%
Binomial	t	67%
Poisson	PLN	76%
Binomial	PLN	17%
Poisson	$PLN > 3$	95%
Poisson	$PLN \leq 3$	64%

Table 3.3: Goodness-of-fit of Poisson and Binomial distributions.

We use

$$n = \max(y_1, \dots, y_N)$$

for estimation.

A system-wide comparison is summarized in table 3.3. We selected randomly 100 sectors and conditions and evaluated the goodness-of-fit of a Poisson and of a binomial distribution with a χ^2 test. Conditioned on time-of day, a Poisson distribution is accepted in 75 % of the cases and a binomial distribution in 67 %. Conditioned on planned traffic, 76 % of the distributions can be seen as Poisson and 17 % as binomial. When planned traffic > 3 , Poisson distributions are accepted in 95 % of the cases. For $PLN \leq 3$, 64 % of the distributions can be characterized by Poisson distributions.

To conclude, we analyzed three definitions for gaps between the number of planned and realized sector entries. Absolute gaps ($GAP_t = REAL_t - PLN_t$)

fluctuate around 0 throughout the day. Their variance is higher during the day (7-19h) than during the night. No serial correlations have been found. The marginal distributions during the day are symmetric with standard deviations lying in [1.6, 3.2]. The probability of their tails is slightly higher than in Gaussian distributions. Relative gaps ($GAP_t = REAL_t/PLN_t$) fluctuate around 1 throughout the day. The variance is lower during the day (7-19h) than during the night. No serial correlations have been found, neither. The marginal distributions are skewed to the right (skewness lies in [0.8, 1.6]). The distributions of their logarithms have higher probability in the tails and around the center than a Gaussian distribution. As a consequence, log-normal distributions are no candidates for relative gaps. Two simple examples of functional gaps ($GAP_t = f(REAL_t, PLN_t)$) are the real traffic conditioned on time-of-day and on planned traffic. These variables take on positive and discrete values. Their distributions are right skewed, too. They can be characterized with Poisson distributions.

3.3 Occurrence of Gaps

In this section we analyze in more detail the realized traffic in a single sector. We characterize it (i) as a function of time and (ii) as a function of planned traffic.

Function of time

A typical daily pattern is shown in Figure 3.8: few traffic in the morning and night; peak hours around noon and in the late afternoon. We assume that

$$REAL_i \sim Poisson(\mu_i)$$

are independent random variables, a non-homogeneous Poisson process, and let its rate vary as a fourth-order polynomial function of time

$$\log(\mu_t) = \sum_{i=0}^4 \alpha_i t^i$$

Given N observations $\mathbf{real} = (real_1, \dots, real_N)$, the parameters α_i are estimated by maximizing the likelihood

$$l(\alpha \mid \mathbf{real}) = \sum_{i=1}^N (real_i \log(\mu_i) - \mu_i)$$

The first derivative results in non-linear equations in the α_i 's, which can be solved with a Newton procedure. This likelihood is a concave function, leading to unique parameter estimates [Cameron and Trivedi, 1998]. Care has to be taken with the statistical properties of these estimates. Consistency and asymptotic normality can be derived by various convergence assumptions of the covariates [Fahrmeir and Tutz, 2001]. These are usually fulfilled in i.i.d. data, but violated for trending regressors. Moreover, these assumptions are more restrictive in the case of dependent data since it usually contains less information than i.i.d data. Stationarity and ergodicity of the covariate process are often assumed, but weaker conditions exist for special cases [Fahrmeir and Tutz, 2001]. As a consequence, we will not make formal inferences about estimated parameters. We will only compare relative goodness-of-fit of various models.

The fitted polynomial is the bold line in Figure 3.8. It captures the low traffic density during night and the two daily peaks. But such a time-trend cannot be justified physically. Moreover, wrong time trend models imply spurious correlation in the residuals [Diggle, 1990]. This is an example of the limitations of a pure data-driven approach. Note that there are many possibilities to model time effects, for example with harmonic curves or with seasonal models.

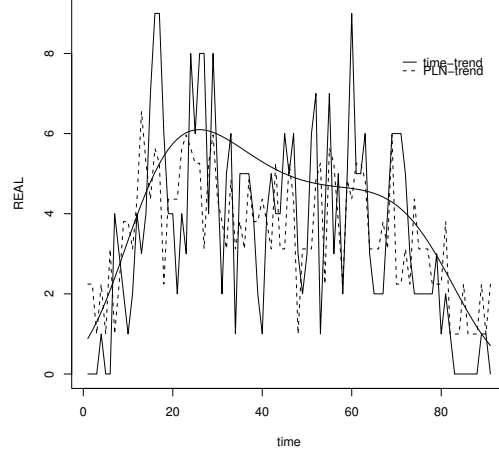


Figure 3.8: Arrivals in fifteen minutes intervals with t^4 time-trend (bold).

Function of planned traffic

We are more interested in the relationship f between the number of planned and real arrivals. In other words, we are looking for a trend that is not a function of time but a function of planned traffic:

$$\mathbf{E}(REAL_t) = f(PLN_{-\infty}, \dots, PLN_{\infty})$$

The variables on the right side have an impact on the variables on the left side. Such an asymmetric relationship between several processes is called ‘transfer function model’ or ‘open-loop system’ e.g. [Kendall, 1989], [Diggle, 1990]. Main tools for the identification of a linear transfer function between stationary processes are cross-correlation and cross-spectrum. One class of non-stationary models for which standard techniques can be applied are series with polynomial time trends. Such trends can be removed by differencing the series, which results in a stationary series e.g. [Kendall, 1989]. These tools are not applicable in our case because we cannot justify a polynomial time-trend.

Figure 3.9 shows the scatterplot of PLN_t against $REAL_t$ on a 15 min timescale. The range of both variables is [0,15]. The sample conditional mean is

$$\hat{\mu}(REAL_t | PLN_t = k) = \frac{1}{n_k} \sum_{PLN_i = k} real_i$$

where n_k is the number of observations with $PLN_t = k$. As a function of k , it

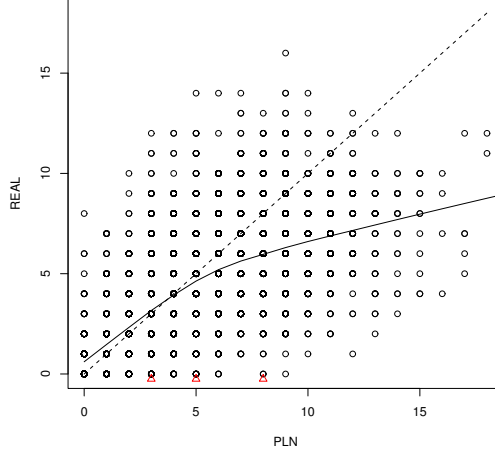


Figure 3.9: Scatterplot of PLN_t against $REAL_t$ (15 min). x axis: number of planned entries, y axis: number of real entries. Bold line: sample means.

has a logarithm-like shape (bold line). The quartiles

$$\{x : P(PLN_t \leq x) = p, \quad p_i \in \{0.25, 0.5, 0.75\}\}$$

are plotted by the red triangles on the level $y = 0$. The sample mean is above the diagonal until the 50% quartile, and falling below it, then. In particular at $PLN_t = 0$, the mean is > 0 .

Three simple descriptions of this relationship are $f(x) \in \{\log(x), \sqrt{x}, 1 - 1/x\}$. Since the variable $REAL_t$ is a count, we assume

$$\log(\mu_t) = \alpha f(PLN_t) + \beta$$

with $\alpha, \beta \in \mathbb{R}$. Note that the model using the logarithmic trend can also be written as the power of α . The predicted mean values of the three models are superposed in Figure 3.10. They all describe accurately the sample means.

To validate this result on a system-level, we fit every candidate model to 30 randomly selected sectors and days. Table 3.4 shows mean values and standard deviations of deviance D and AIC of every model. The first two models are baseline models; the homogeneous Poisson process and a non-homogeneous Poisson process with rate $\log(\mu_t) = \alpha PLN_t + \beta$. Average deviance (AIC) are 213.5 (527.0) and 140.5 (434.5) on 95 and 94 degrees of freedom. Models 3-5 are the candidates for the observed trend in Figure 3.10: $\log(\mu_t) = \alpha \log(PLN_t) + \beta$, $\log(\mu_t) = \alpha \sqrt{PLN_t} + \beta$ and $\log(\mu_t) = \alpha(1 - 1/PLN_t) + \beta$. Their deviances are

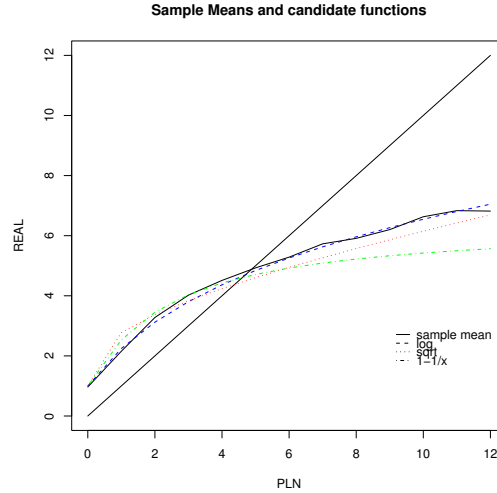


Figure 3.10: Relationship between number of planned arrivals PLN (x-axis) and average number of real arrivals $REAL$ (y axis) in 15 minutes time intervals.

all ~ 117 (425), so the baseline models are inappropriate. The last model is the polynomial time trend $\log(\mu_t) = \sum_{i=0}^4 \alpha_i t^i$. Its average deviance is 118.6 on 91 d.f. The use of more parameters is reflected in an AIC of 442.4, which is higher than the AIC for the candidate models. The variation of the statistics over all 30 sectors lies in the range $\pm 10\%$. Thus, independently of sector and day, the three candidate models all explain a large part of the variation in the data.

To summarize, the process $REAL_t, t = 1, 2, \dots$ varies over time. We described this variation as a non-homogeneous Poisson process with rate as a function of time and as a function of planned traffic. As a function of time we used a polynomial that captures the night/day traffic variations. As a function of planned traffic we first looked at the sample conditional mean of realized traffic given planned traffic. We then compared the goodness-of-fit of three candidate functions for this relationship. All models describe equally well the variation in the data. But these findings are empirical. We found ways to accurately *describe* the data. The question is not whether one description predicts better than another. We should explain *why* the data shows this behavior before drawing further conclusions.

Model	$\mu(\mathbf{D})$	$\sigma(\mathbf{D})$	$\mu(\mathbf{AIC})$	$\sigma(\mathbf{AIC})$	d.f.
1	213.5	41.2	527.0	53.9	95
<i>PLN</i>	140.5	17.9	434.5	40.8	94
$\log(\textit{PLN})$	118.2	17.7	428.0	32.0	94
$\textit{sqrt}(\textit{PLN})$	117.1	20.3	422.2	35.0	94
$1 - 1/\textit{PLN}$	117.9	14.9	419.3	34.5	94
$\sum_{i=0}^4 t^i$	118.6	18.4	442.5	27.1	91

Table 3.4: Goodness-of-fit of different trend models.

3.4 Propagation of Gaps

Obviously, a gap between planned and real number of entries in a sector S at time t propagates to its neighboring sectors at time $t+1$, because aircraft cannot stand still. On the other hand, pilots and air traffic controllers can compensate gaps by re-routing or speed adjustments of aircraft. In this section we analyze how such gaps propagate in reality through the airspace. Are there systematic movements of gaps or do controllers compensate them successfully?

We consider $Z_t = [Z_{1t}, Z_{2t}, \dots, Z_{mt}]'$, $t \in \mathbf{Z}$ as a random process where Z_{it} represents the gaps between planned and realized traffic in sector i in time-slot t . Our aim is to study the correlation structure of the process. This is the first step in every analysis of multiple time series [Kendall, 1989] or more generally in graphical modeling. Here, recent similar work can be found in the analysis of gene-network structures where interactions between a large number of genes are sought [Brillinger and Villa, 1997], [Schäfer and Strimmer, 2005]. More formally, we are concerned with the problem of inference about high-dimensional random matrices. We will address the problem of sample size, dependencies between coefficients and spurious correlations.

This section contains two results: first, we derive three bounds for the variability of the coefficients of the correlation matrix. The approaches are analytical (based on central limit theorem) and numerical (bootstrap technique). Secondly, we identify patterns in the correlation structure of the most congested part of the airspace. We show evidence that no systematic re-routing takes place in the sector network.

Visualization

Before analyzing the correlations, we visualized the propagation of gaps between planned and realized traffic in a movie (Figure 3.11). For all sectors, the series

$GAP_t, t = 1, 2, \dots$ is visualized with the colors

$$GAP_t = \begin{cases} \text{green} & REAL_t < 90\% \text{ of } PLN_t \\ \text{yellow} & REAL_t < \pm 10\% \text{ of } PLN_t \\ \text{red} & REAL_t > 110\% \text{ of } PLN_t \end{cases}$$

In the visualization no eye-striking propagation patterns are visible. We conclude that a more detailed analysis is necessary.

Inference for correlation matrices

In this part we define the correlation matrix between multiple time series and its sample version. We then discuss general problems of inference before deriving bounds for the variability of the sample coefficients.

Let $Z_t = [Z_{1t}, Z_{2t}, \dots, Z_{mt}]', t \in \mathbf{Z}$ be an m -dimensional jointly stationary vector process with mean vector

$$\mathbf{E}(Z_t) = \boldsymbol{\mu} = \begin{bmatrix} \mu_1 \\ \mu_2 \\ \vdots \\ \mu_m \end{bmatrix}$$

and cross-covariances between $Z_{i,t}$ and $Z_{j,s}$ that are functions of the time difference $(s - t)$ for all $i, j = 1, \dots, m$. Its covariance matrix function is

$$\begin{aligned} \boldsymbol{\Gamma}(k) &= Cov\{Z_t, Z_{t+k}\} = \mathbf{E}[(Z_t - \boldsymbol{\mu})(Z_{t+k} - \boldsymbol{\mu})'] \\ &= \mathbf{E} \begin{bmatrix} Z_{1t} - \mu_1 \\ \vdots \\ Z_{mt} - \mu_m \end{bmatrix} [Z_{1t} - \mu_1, Z_{2t} - \mu_2, \dots, Z_{mt} - \mu_m] \\ &= \begin{bmatrix} \gamma_{11}(k) & \gamma_{12}(k) & \dots & \gamma_{1m}(k) \\ \vdots & \vdots & \dots & \vdots \\ \gamma_{m1}(k) & \gamma_{m2}(k) & \dots & \gamma_{mm}(k) \end{bmatrix} = Cov\{Z_{t-k}, Z_t\} \end{aligned}$$

where

$$\gamma_{ij}(k) = \mathbf{E}[(Z_{it} - \mu_i)(Z_{j,t+k} - \mu_j)] = \mathbf{E}[(Z_{i,t-k} - \mu_i)(Z_{j,t} - \mu_j)]$$

For $i = j$, $\gamma_{ii}(k)$ is the autocovariance function for the i th component process Z_i . Else, it is the cross-covariance function between components Z_i and Z_j .

The correlation matrix function is defined by

$$\boldsymbol{\rho}(k) = \mathbf{D}^{-1/2} \boldsymbol{\Gamma}(k) \mathbf{D}^{-1/2} = [\rho_{ij}(k)]$$

for $i, j = 1, 2, \dots, m$ where \mathbf{D} is the diagonal matrix in which the i th diagonal element is the variance of the i th process:

$$\mathbf{D} = diag[\gamma_{11}(0), \gamma_{22}(0), \dots, \gamma_{mm}(0)]$$

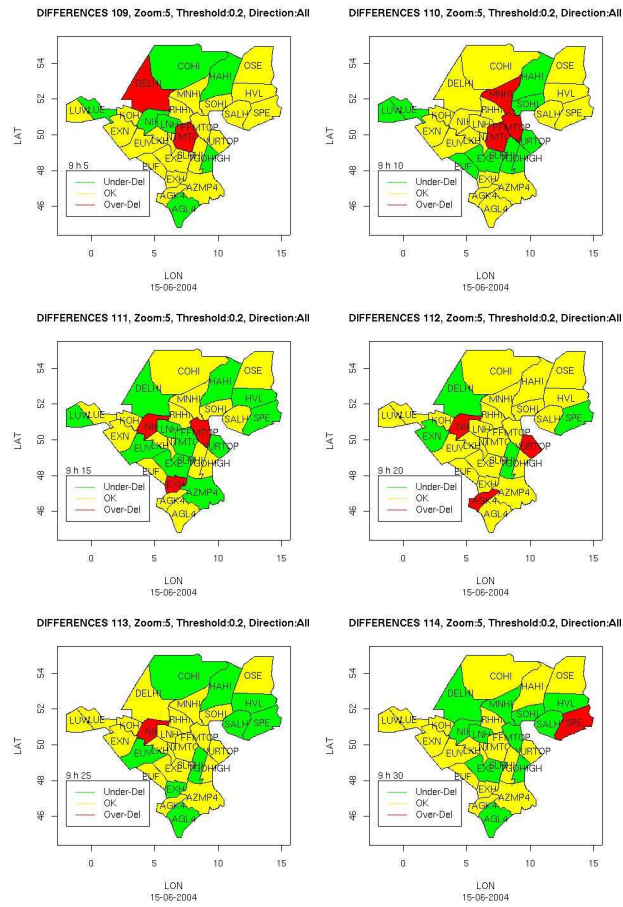


Figure 3.11: 30 minutes evolution of traffic. Congestion appears ‘randomly’. Red: over-delivery, green: under-delivery, yellow: no difference between planned and executed traffic

For example, the off-diagonal elements of $\rho(k)$

$$\rho_{ij}(k) = \frac{\gamma_{ij}(k)}{[\gamma_{ii}(0)\gamma_{jj}(0)]^{1/2}}$$

represent the cross-correlation functions between the processes Z_i and Z_j .

Estimation

The standard estimators of covariance and correlation matrices are sample-covariance and sample-correlation. The sample covariance matrix has elements

$$\hat{\gamma}_{ij}(k) = \frac{1}{n-k} \sum_{t=1}^{n-k} (Z_{it} - \bar{Z}_i)(Z_{j,t+k} - \bar{Z}_j)$$

where

$$\bar{Z}_i = \frac{1}{n} \sum_{t=1}^n Z_{it}$$

are the component-wise sample means. The sample correlations are then

$$\hat{\rho}_{ij}(k) = \frac{\hat{\gamma}_{ij}(k)}{[\hat{\gamma}_{ii}(0)\hat{\gamma}_{jj}(0)]^{1/2}}$$

These estimators are asymptotically normally distributed [Kendall, 1989]. Modifications exist to address issues of bias and positive definiteness [Kendall, 1989]. [Ledoit and Wolf, 2004] and [Schäfer and Strimmer, 2005] recently studied the estimation of high-dimensional covariance matrices. They propose James-Stein estimators to minimize further mean squared error and to obtain positive definite and invertible matrices. A disadvantage of their approach is that the sample properties of their estimators are not known.

Sample Variability

Our objective is to decide whether the coefficients of the correlation matrix differ significantly from 0. For this, the variance of the sample correlations has to be known. For large sample size n the variance of a single sample correlation coefficient under the hypothesis that the true correlation is 0 is $\frac{1}{\sqrt{n-1}}$ [Saporta, 2006]. The elements of a sample covariance matrix are not independent of each other. Thus, sequential tests are not appropriate. As far as the sample covariance matrix is concerned, exact distributions and tests, e.g. the identity with a given matrix, are available [Anderson, 1958]. These results generally require assumptions of normality of the parent variables because, even with independent observations and large sample sizes, fourth-order moments determine the relationship between the elements of the sample covariance matrix since a fraction of the estimates comes from a single vector observation — which has some unknown joint distribution. When observations are dependent, the situation gets more complicated. In large samples and for stationary time-series, a result from Bartlett is then usually used [Kendall et al., 1983]. It can be used to show that when the series $Z_i(t), Z_j(t)$ are uncorrelated,

$$V[\hat{\rho}_{ij}(k)] = \frac{1}{n-k} \sum_{s=-\infty}^{\infty} \rho_{ii}(s)\rho_{jj}(s) \quad (3.3)$$

and

$$Cov[\hat{\rho}_{ij}(k), \hat{\rho}_{ij}(k+l)] = \frac{1}{n-k} \sum_{s=-\infty}^{\infty} \rho_{ii}(s)\rho_{jj}(s+l) \quad (3.4)$$

This means that even for large n (and under the assumption of normality), the variance and covariance of the sample correlations depend on all correlations of the original process. Thus it is impossible to estimate these quantities directly from a finite sample. In practice, approximations are usually used, for example by assuming that the individual series correspond to white noise (for example after pre-whitening).

In what follows, we derive bounds for $V[\hat{\rho}_{ij}(k)]$. These can be used as a heuristic in the analysis of the correlation matrix. We use Bartlett's formula to compute realistic variances taking into account serial correlation between observations. Then we use a re-sampling approach to estimate the real sample variability.

To account for dependencies between successive observations, we calculate the variance inflation for several dependency structures compared to independent observations due to Bartlett's formula 3.3. The dependency structures are the following:

$$\rho_{ii}(s) = \rho_{jj}(s) = \begin{cases} \rho_{max} & s < l_{max} \\ 0 & else \end{cases}$$

Under this structure, equation 3.3 becomes

$$V(\hat{\rho}_{ij}(k)) < \frac{1}{n-k} \sum_{s=-\infty}^{\infty} \rho_{ii}^2(s) = \frac{1}{n-k} (1 + 2l_{max}\rho_{max}^2)$$

The table below shows $nV(\hat{\rho}_{ij}(1))$ for different values of ρ_{max} and l_{max} :

$l_{max} \backslash \rho_{max}$	0.01	0.05	0.1	0.2
10	1.002	1.05	1.20	1.8
75	1.015	1.375	2.50	7.0
100	1.02	1.50	3.00	9.0
150	1.03	1.75	4.00	13.0

We can expect 30 - 70 % increase of variance with respect to independent realizations.

Finally, we evaluate $V(\hat{\rho}_{ij})$ non-parametrically, with a block-bootstrap [Bühlmann, 2002]. We select the block-size = 288 (corresponding to 1 day) and re-estimate $\hat{\rho}_{ij}(1)$ 200 times based on independently drawn samples with replacement. The results are shown below:

n	288	2*288	10* 288
$s.e(\hat{\rho}_{ij})$	0.12	0.08	0.04
$\hat{s}e(\hat{\rho}_{ij})$	0.14	0.1	0.05

where the first line is the standard error obtained from Bartlett's formula under the assumption of white noise and the second line the bootstrap estimation of the standard error. It shows an increase of 10 %, so if the true dependency structure can be modeled by a stationary time series, then the dependencies are very weak.

To summarize, we computed two bounds for the variation of the sample coefficients in a large dimensional correlation matrix. The first bound took into account the serial dependencies between observations, but assumes stationary generating mechanisms. The second one released the assumptions by a re-sampling technique, resulting in a numerical value giving few analytical insight in the problem. In the context of our problem — 31 processes, 36 time-slots, 91 days of data — we summarize (i) that the large sample size decreases the standard errors to values close to 0 and (ii) the bounds give similar values between [0.1,0.2]. We conclude that correlations below 0.2 should be interpreted with suspicion and remind that the interesting part in the analysis of auto- and cross-correlations is the discovery of 'global patterns' rather than of single significant coefficients [Diggle, 1990].

Results

We analyzed correlations between 31 sectors in the Central European Airspace, covering London, Zurich and Berlin.

More formally, we consider the 31 dimensional vector of random processes $\mathbf{GAP}_t = \mathbf{PLN}_t - \mathbf{REAL}_t, t \in \mathbb{R}$, where the i th component $GAP_{i,t} = PLN_{i,t} - REAL_{i,t}$ represents the gaps between the planned and realized number of entries in sector i . The process is observed in 5 minutes time intervals, leading to 288 samples per day. In total, 91 week-days are available (Mon-Thu) in the summer period 13.5.- 29.9.2004. The data takes the form $\{\mathbf{gap}_t^d\}_{d=1}^N, 1 \leq t \leq 288, N = 91$.

The correlation matrix function for all 31 sectors was estimated up to lag $k = 36$, corresponding to 3 hours. This corresponds to $d=31 * 36=116$ components to be estimated.

Figure 3.12 visualizes the results. An arrow between two sectors (i, j) represents a significant correlation at at least one lag k . Positive and negative lags have opposite arrows. Local correlations (from one sector to a direct neighbor) are drawn in red. They reproduce almost the route network. For example, in the central flow (Frankfurt-London), they are bi-directional, whereas in the flow from Zurich to London, they are mono-directional. Non-local correlations (from one sector to a sector beyond the direct neighborhood) are plotted in green. They reproduce only routes with high traffic densities. No correlations between two sectors that are not connected by a route are found.

We now analyze in more detail the sector LNH and two of its neighbors, NIH and RHHI (light Grey region in Figure 3.12). The arrow between LNH and NIH is bi-directional, so there is correlation on positive and on negative lags. No arrow is plotted between LNH-RHHI and NIH-RHHI. Figure (3.13) shows the estimated correlation matrix function of these three sectors. The diagonal elements correspond to the autocorrelations. All three show no significant correlations. The off-diagonal elements display the cross-correlations for positive lags in the upper diagonal $\rho(GAP_{it}, GAP_{j,t+k})$ and negative lags in the lower diagonal $\rho(GAP_{it}, GAP_{j,t+k})$. The coefficients at lag 1 and -2 between LNH and NIH are the only significant correlations.

For more insight into non-local correlation, we analyze the two dark Grey sectors EXH and EUY in Figure 3.12. They are separated by the two sectors EUF and EXE. Figure 3.14 shows the correlation matrix function between EXH and EUY. Again, the pattern of autocorrelation in the diagonal elements shows a decay, starting from a negative value. But none of them are significant. The only significant correlation is at lag -5, corresponding to the average traversal time.

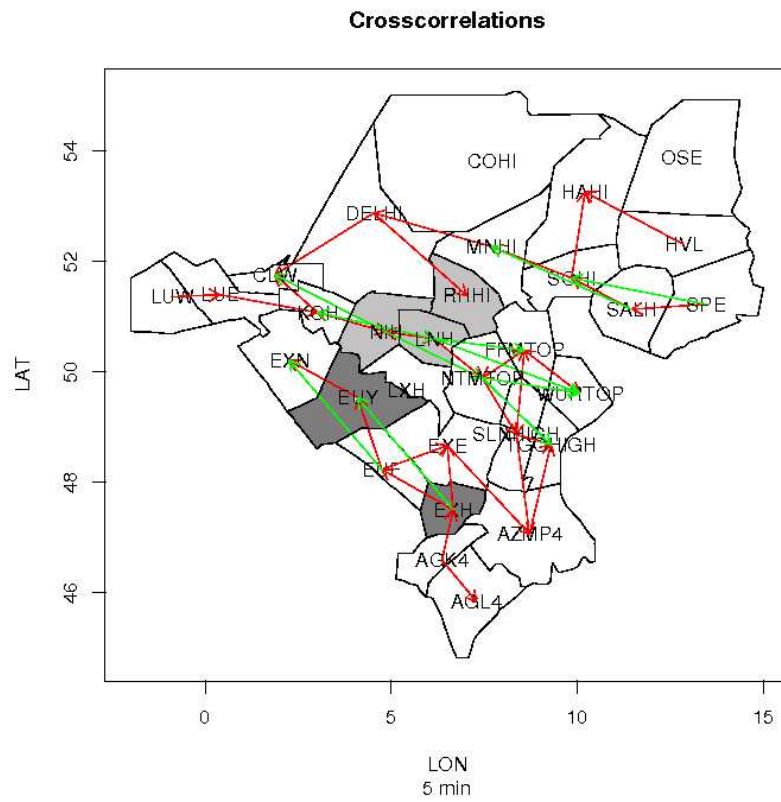


Figure 3.12: Visualization of the cross-correlation matrix.

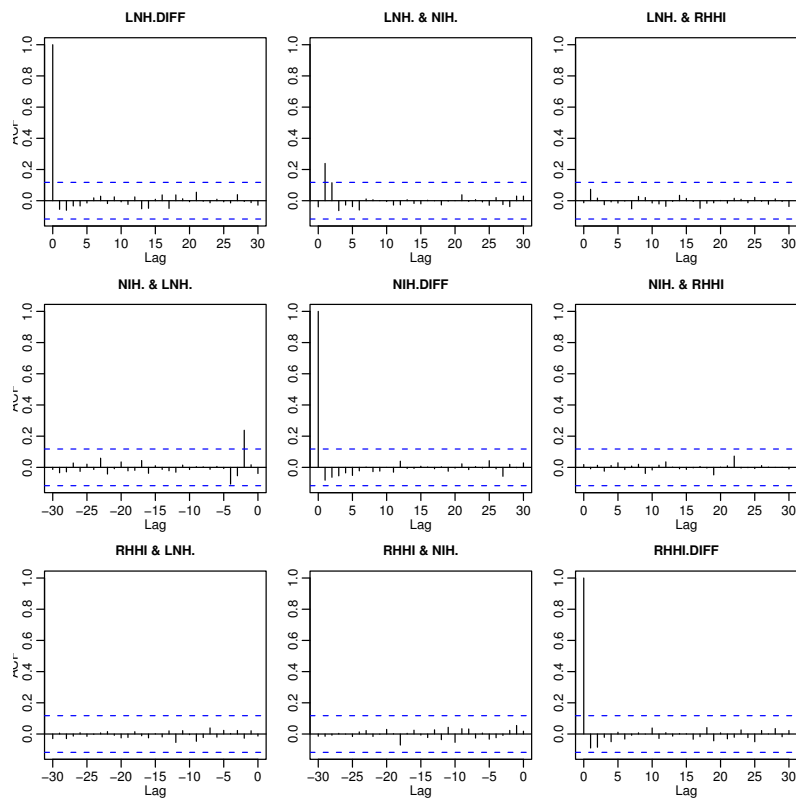


Figure 3.13: Cross-correlation matrix between sectors LNH, NIH and RHHI (local neighbors, light gray area).

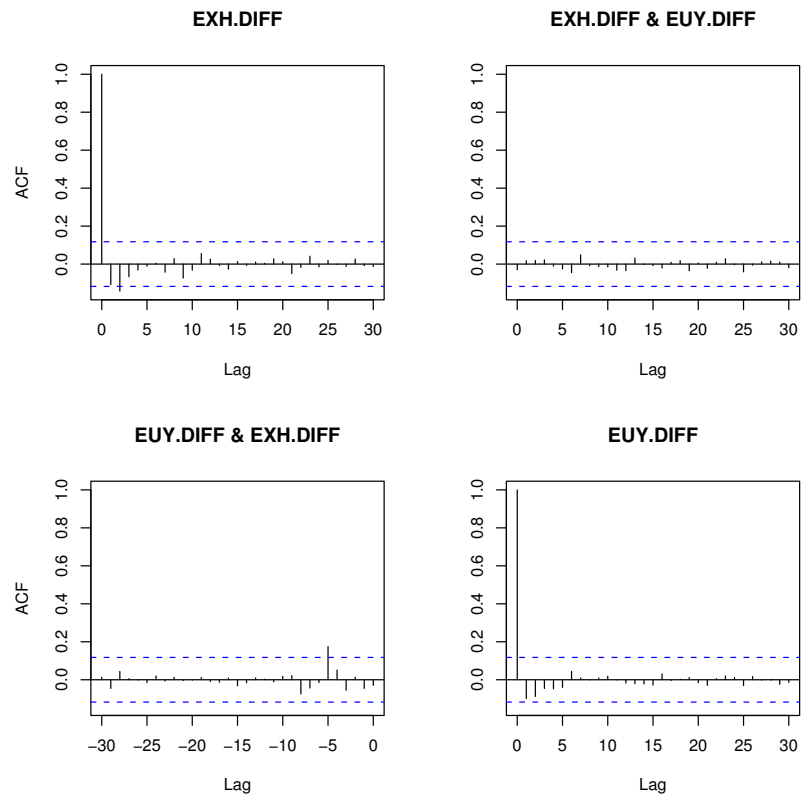


Figure 3.14: Cross-correlation matrix between sectors EXH and EUY (non-local neighbors, dark Grey area).

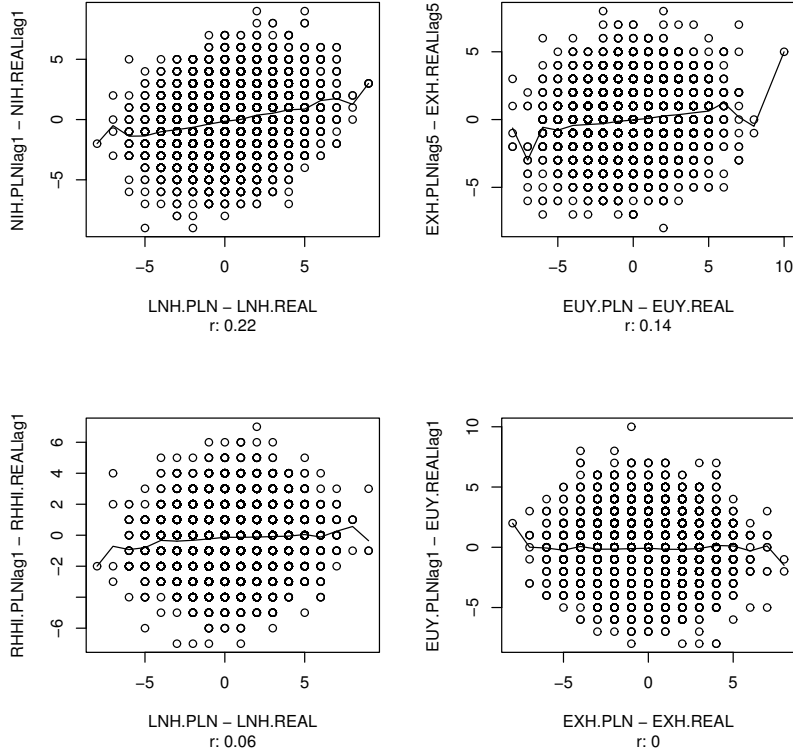


Figure 3.15: Scatterplots of gaps in one sector against time-lagged gaps in other sectors.

We expect that gaps above average in one sector lead at least approximately to gaps above or below average in another sector. For this reason we use linear correlation as measure of dependency. Correlation expresses dependency in average between two random variables X and Y : for fixed $X = x$, the average $\mathbf{E}(Y)$ is a function of x . Linear correlation is the special case when this dependency is approximately linear. Figure 3.15 shows 4 scatter plots of variables in the system. In each panel the bold line is the sample mean. It is reasonably linear. No other functional form of dependency is visible, neither. The two upper ones have significant coefficients of linear correlation. The two lower ones have not. Thus, linear correlation as a measure for dependence seems justified, even if the dependency between the variables is visibly weak.

Figure 3.16 summarizes the significant correlations of the full 31×31 correlation matrix function. All correlation coefficients are positive. Local correlations

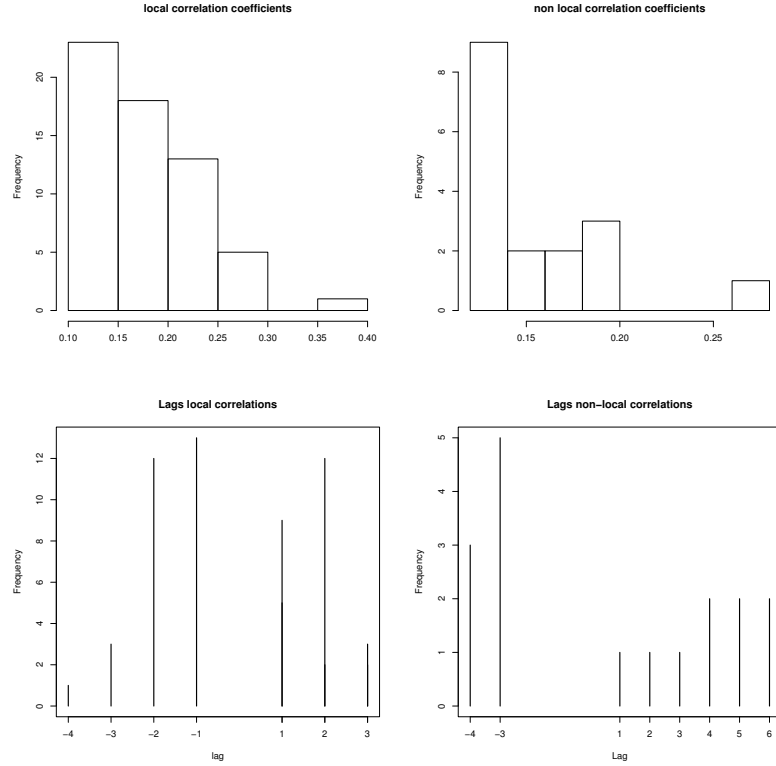


Figure 3.16: Summaries of coefficients of the complete cross-correlation matrix.

are on average 0.19 and have a maximum of 0.34 (top left) The non-local correlations are on average 0.16 and have a maximum of 0.24 (top right). Local correlations occur between lags -4 and 3 (bottom left). This lies in the range of expectation since the traversal time for one sector lies between 6 and 10 minutes. Figure 3.17 shows the strength of correlation as a function of lag for local correlations. On the x-axis, the lag is plotted. On the y axis, the corresponding correlations. The highest correlations occur at lags [-2,2]. Correlations on lags -3 and 3 occur between sectors ‘CLW-DELHI’, ‘DELHI-RHHI’, ‘EUY-EUF’ and ‘AZMP4-SLNHIGH’ which are all huge sectors. The only unexpected high correlation (0.22) between ‘SALH-SOHI’ on lag 3 can be disregarded, because of the sample variance of the coefficients. The correlation at lag -4 has strength 0.12 and can be disregarded for the same reason. Non-local correlation coefficients occur up to lag 6, corresponding to the average traversal time (bottom right).

From those neighbors of sectors that are correlated, 77 % have exactly one significant coefficient, 19 % have two and 4 % three or four (Figure 3.18, top).

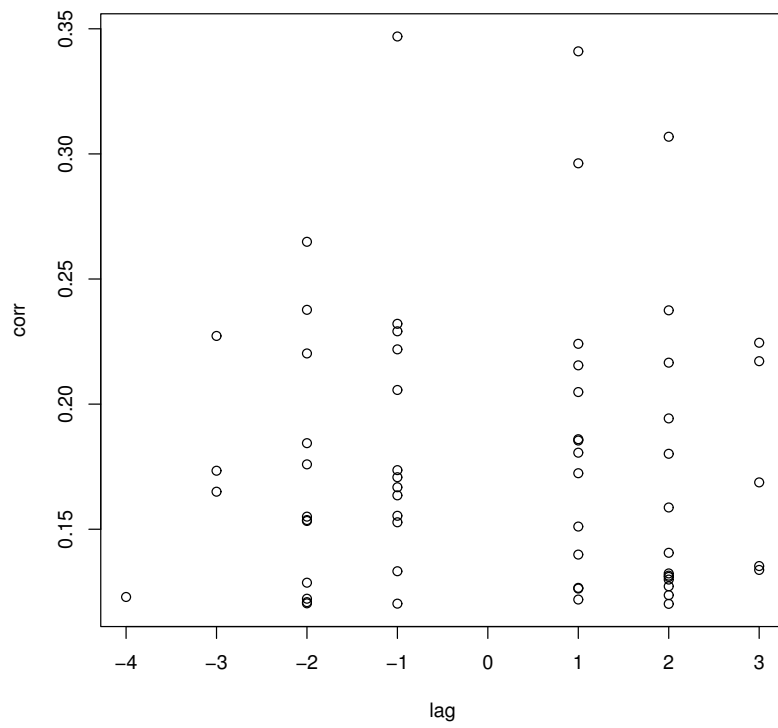


Figure 3.17: Strength of correlation as a function of lag (local correlation).

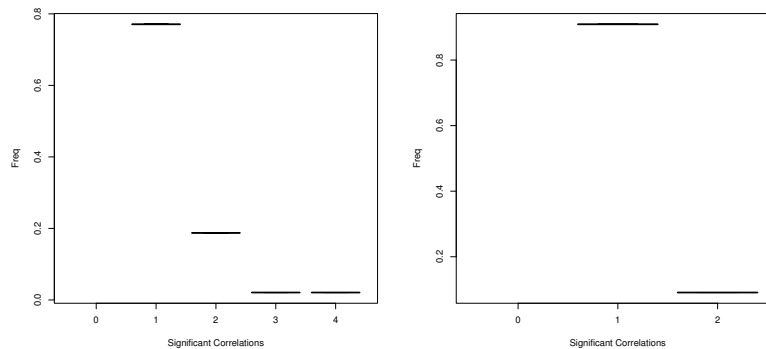


Figure 3.18: Distribution of the number of significant coefficients between correlated sectors.

For non-local correlated sectors, 91 % have exactly one and 9 % have two significant coefficients (Figure 3.18, bottom). This suggests that the correlation structure in the system (i) does not appear to contain spurious correlations and (ii) has an intuitive explanation.

3.5 Validation

Aggregation

Figure 3.19 shows the relationship between PLN_t and $REAL_t$ on three different time-scales (5 min, 15min, 60 min). On all scales the relationship is logarithm-like.

Generalization

Figure 3.20 shows the relationship between PLN_t and $REAL_t$ for 12 sectors from Central Upper Airspace (15 min. time-scale). They all show the same logarithm-like shape. The fluctuations at the end of the intervals can be explained by few underlying data. For all the 31 sectors, 68 % of the asymptotes lie in the interval $(8, 10]$. Since we are working with 15 minutes intervals, this corresponds to hourly workloads between 36 and 40 aircraft. This is roughly the declared capacity of many sectors. 26 % lie below and 6 % above this interval. In 63 % of the cases, the points, where $PLN = REAL$ lie between $6 \leq PLN < 8$. In 35 % of the cases, these points are below 6. Only in one case, the point where PLN equals $REAL$ lies above 8.

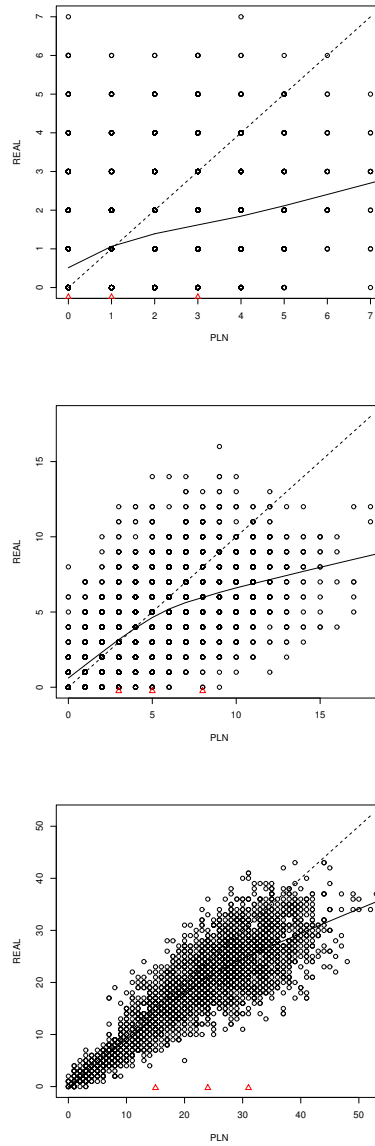


Figure 3.19: Scatterplots of PLN_t against $REAL_t$ on three different timescales 5 min (top), 15 min (middle) and 60 min (bottom).

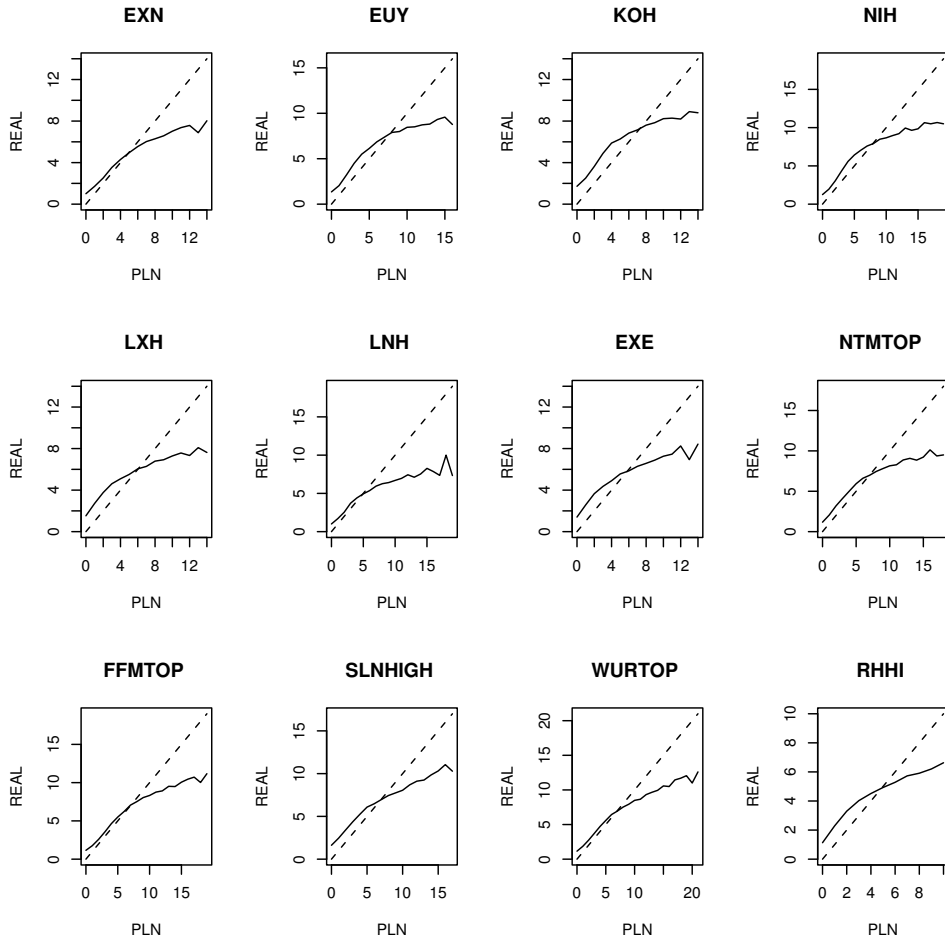


Figure 3.20: Plot of sample means in randomly chosen sectors.

3.6 Interpretation

Uncertainty

We analyzed three definitions of gaps between the number of planned and realized entries in a sector.

We observed that the planned and the realized traffic patterns are similar and that they repeat on a daily basis. We also noted that the patterns are sector-specific: some sectors have clear peaks twice a day, others have constant traffic densities. This is known by ATM experts: sectors close to airports have constant workload, others are affected by trans-Atlantic jet streams and have a peak in the early morning. Thus, the traffic pattern of a sector depends on different parameters. In contrast to this, absolute $PLN_t - REAL_t$ and relative $PLN_t/REAL_t$ gaps fluctuate around 0 and 1 and have constant variance during the day and during the night. This suggests that the phenomenon of gaps is time-invariant (stationary during the day (7-19h)). In particular, no peak hours of gaps exist.

We then analyzed the marginal distributions of the three definitions during the day (7-19h).

1. $REAL_t - PLN_t$ (absolute definition)

Absolute gaps are symmetrically distributed with $\mu \sim 0$ and $sd \sim 3$. This means that roughly the same number of aircraft than planned arrives at sector entries. It also means that in 96 % of the cases, ± 6 of the planned aircraft arrive. The tail probabilities are slightly higher than for Gaussian distributions. Gaussian distributions can be expected when uncertainty factors are independent from each other.

2. $REAL_t/PLN_t$ (relative definition)

Relative gaps are distributed asymmetrically around $\mu \sim 1$. One reason is that the variable is positive by definition and that the mean is close to 0, so it is 'cut-off' on the negative values. The logarithm disagrees clearly with a Gaussian distribution: the tails and the center contain higher probabilities than Gaussian distributions. Thus, the original variable is not log-normal distributed, which would be the case if the uncertainty factors were independent but with multiplicative effect. Possible interpretations are heterogeneity (different types of behavior) and dependence between uncertainty factors in the data.

3. $REAL_t = f(PLN_t, t)$ (functional definition)

Gaps as a function of time or planned traffic are distributed asymmetrically. Poisson distributions accurately characterize this representation of gaps. This gives an idea of the variation of the number of arrivals in a sector because mean and variance are the same for a Poisson distribution. The Poisson distribution can be derived analytically from counting the

number of events in larger time intervals when the probability of occurrence of events are constant and independent over time, characterizing ‘total randomness’. Moreover, Poisson distributions are the limiting distributions when several Point processes are superposed [Cox and Isham, 1980]. But one cannot deduce from an observed Poisson distribution that the probability of events is constant and independent [Daley and Vere-Jones, 1988]. Moreover distributions with similar shape exist (e.g. negative binomial distribution), implying different physical interpretations. To conclude, it is not enough information to unambiguously draw conclusions about the underlying mechanism of the phenomenon [Daley and Vere-Jones, 1988]. This point will be investigated in more detail in the next chapter.

Occurrence

We described the variation in the arrival process as a non-homogeneous Poisson process with rate as a function of time and as a function of planned traffic. As a function of time we used a polynomial that captures the night/day traffic variations. As a function of planned traffic we first looked at the sample conditional mean of realized traffic given planned traffic. We then compared the goodness-of-fit of three candidate functions for this relationship. All models describe equally well the variation in the data. But these findings are empirical, and we should explain *why* the data shows this behavior before drawing further conclusions.

Propagation

We showed that propagation between gaps occurs on two levels: (i) locally, that is between a sector and its direct neighbors and (ii) globally on ‘traffic highways’, that is between two sectors that are connected through a flight route with high traffic densities. No unexpected correlations are found. This is evidence that controllers do not systematically re-route traffic flows to absorb gaps.

Conclusion

We conclude that gaps between the number of planned and realized traffic (i) occur systematically (ii) that their size can be described by Poisson distributions and (iii) that they propagate through the airspace in an expected way. These findings are empirical. We found an accurate *description* of the data and its variation. But the question is not whether one description ‘performs better’ than another. The question is why the data shows these characteristics. An analysis of the mechanisms that lead to gaps between planned and realized traffic has to be done.

Chapter 4

Results of Probabilistic Analysis

We analyze the phenomenon of gaps between the number of planned and the number of real entries into flight sectors. The approach in the previous chapter was exploratory: we did not make assumptions about the phenomenon because we wanted to identify unexpected characteristics of it. And it was macroscopic: we analyzed the number of aircraft entering sectors in given time intervals because it corresponds directly to the definition of gaps. We concluded that gaps between the number of planned and realized aircraft do occur systematically, that they propagate in an expected way through the system, and that the uncertainty about the size of these gaps can be characterized by Poisson distributions.

In this chapter we analyze the reasons for this. This time, the approach is probabilistic: we make assumptions about the behavior of users of the system. And it is microscopic: we analyze the sector-entry times of aircraft and events that disturb them. This serves to interpret the results of the first part.

Mechanisms of gaps between planned and realized traffic

Our starting point is that the flow planning procedure assigned departure slots to every aircraft. This means that the initial flight plans $(S_1, t_1), \dots, (S_n, t_n)$ have been regulated into $(S_1, t'_1), \dots, (S_n, t'_n), t'_1 \geq t_1$ with possibly delayed departure times t'_1 . Since slot allocation takes place at least two hours before the intended take-off time, the air-traffic controllers can anticipate the amount of traffic in their sectors over time.

Figure 4.1 shows three events that disturb the flow planning

- Cancellation and rerouting: some of the scheduled flights are canceled or rerouted to other sectors.

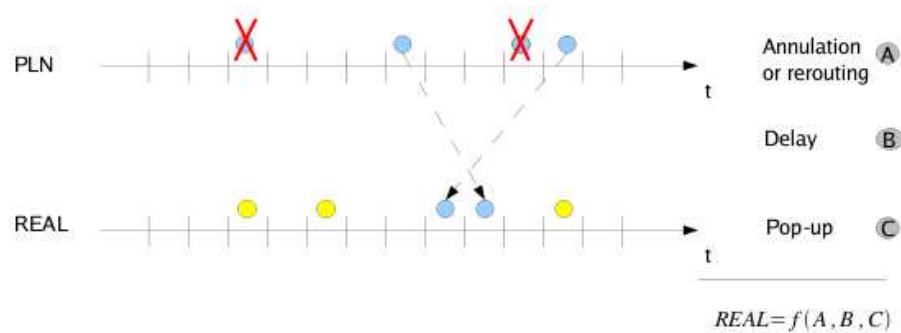


Figure 4.1: Events at a sector entry.

- Delay: aircraft arrive too early or too late at the sector. Delay occurs either at the departure airport or during the flight.
- Pop-up: rerouted aircraft from other sectors or aircraft without submitted flight plans arrive.

It is natural to think that random events deviate flights from their flight plans. For example, weather conditions or unpredictable events (e.g. passenger delay or technical failure) constantly affect the system. One likes to assume that such event do not disturb the flow planning systematically. In average, their effects should be canceled out.

On the other hand there are mechanisms that systematically disturb the flight plans. For example, airlines use the cancellation of flights as a strategy to avoid high departure delays [Mukherjee et al., 2005]. Or departure delays are often caused by delayed connecting flights, which can propagate over the whole network [EUROCONTROL, 2002]. Moreover, there are different departure strategies, five minutes before- or ten minutes after the scheduled departure slot [EUROCONTROL, 2002].

In this part of the thesis we analyze conditions for the *systematic occurrence* of gaps between the number of planned and realized aircraft. We restrict this general question to an analysis of the the question ‘What is the impact of random disturbances on the flow planning?’. If gaps are exclusively caused by random disturbances, they are a natural, and unavoidable characteristic of the system. If not, non-random forces apply to the system and the occurrence of gaps might be controllable.

Methodology

We are working with stochastic Point processes subject to random disturbances. We derive characteristics of the relationship between such processes. Compared to the first part of the thesis, we formulate more precise hypotheses. This allows us to make deductions about the phenomenon.

Formalization

More formally, we analyze the model:

$$\tau'_i = \tau_i + \epsilon_i, i \in \mathbb{N} \quad (4.1)$$

with

- τ'_i : observed arrival time of aircraft i ($\in \mathbb{R}$)
- τ_i : planned arrival time of aircraft i ($\in \mathbb{R}$)
- ϵ_i : disturbance of aircraft i (a continuous random variable)

to answer two questions: (i) what is the relationship between the processes $\{\tau'_i\}$ and $\{\tau_i\}$ when the disturbances ϵ_i occur completely at random ? And (ii) how do these disturbances look like in reality?

Related work

[Wanke et al., 2004] decompose sector demand uncertainties into the same three categories ‘cancellation, delay and pop-up’ as above. They further subdivide the ‘delay’ component into ‘routing/altitude, departure time and flight progress’. They analyze the distributions of all components, conditionally to external, discrete variables. For example the probability of a pop-up depends on the time-of-day, the day-of-week and of the prediction horizon. More complex distribution models, for example for re-routing, are developed, too. They identify that pop-ups can be described by geometric distribution functions. The same result can be found in [Boghadi, 2002]. The other components do not allow for substantial conclusions.

[Tu et al., 2007] analyze delay distribution of departures. They identify Gaussian mixture distributions with three components for the individual random variables ϵ_i . This can be interpreted with the take-off behavior: either five minutes before, exactly at, or ten minutes after the scheduled departure slot. The result is in harmony with [Constans et al., 2004] who conclude that Gaussian distributions alone are no accurate models for the delays.

[Mukherjee et al., 2005] propose an analytic model for the probability of cancellation at congested airports. Their assumption is that airlines cancel flights when the expected delays exceed a threshold. This is modeled as a maximum

flow problem, where the flows are constrained by the initial demand and the threshold. The probability of cancellation is then the ratio between the maximum flow and the initial demand.

In the same paper, [Mukherjee et al., 2005] describe an analytic model for the en-route delay that is caused by capacity limitations of the arrival airport. Such delay is materialized by air-holdings. They assume a non-homogeneous Poisson process as arrival process and an Erlang distributed runway usage time. Given the hourly demand and capacity profiles, they model the probabilities $P_n(t)$ of having n aircraft in the system at time t , for $n = 0, 1, 2, \dots$. They validate their models in a simulation game with decision makers from the airline industry and conclude that it can be used as a decision tool in the strategic slot allocation procedure.

Chapter outline

The chapter contains two parts. In each part we analyze one aspect of model (4.1). In the first part we consider the disturbances $\{\epsilon_1, \dots, \epsilon_n\}$ as purely random. We show that systematic gaps between planned and realized traffic occur for three classes of flight schedules $\{\tau_i\}$. In the second part we analyze past flight data to reveal the dependency structure of the process $\{\epsilon_1, \dots, \epsilon_n\}$. We identify similarities with time-series models.

4.1 Summary of Results

Complete random disturbances cause gaps

We assume that $\{\epsilon_1, \dots, \epsilon_n\}$ are independently and identically distributed random variables. We analyze the conditional expectation between the two processes $\{\tau'_i\}$ and $\{\tau_i\}$. When $\{\tau_i\}$ is a Poisson process, this expectation is a linear function. When no hypothesis about the arrival process is made, it is non-linear. In both cases, significant differences with the sample data exist. We conclude (i) that gaps between planned and realized traffic have to be expected, (ii) that a logarithm-like shape of the gap-function has to be expected and (iii) that the disturbances are not independently and identically distributed in reality.

Real disturbances do not occur at random

We analyze past flight data of disturbances $\{\epsilon_1, \dots, \epsilon_n\}$ and show that dependencies between successive terms exist in reality. We identify similarities with two linear time-series models. The result is empirical and we give two ideas for further analysis before interpretation.

4.2 Consequences of Independence Assumptions

In this section we analyze the effect of complete random disturbances on flight schedules. For this, we consider the random disturbances $\{\epsilon_1, \dots, \epsilon_n\}$ as independently and identically distributed random variables. We derive analytically and experimentally the relationship between the processes $\{\tau_i\}$ and $\{\tau'_i\}$ under this condition. From this we conclude that (i) systematic gaps between the number of planned and realized traffic are to be expected and (ii) that the disturbances ϵ_i do not occur at random in reality.

Point processes

A sector S has several entry points E_1, \dots, E_{n_S} . For each entry point E_k , a set of aircraft $\{1, \dots, i_k\}$ is planned to enter at times $\{t_1, \dots, t_{i_k}\}$. No more than one aircraft is planned to enter an entry point at a time. Such series of events can be modeled as orderly Point processes [Cox and Isham, 1980], [Daley and Vere-Jones, 1988]. They are continuous time, discrete state space stochastic processes. An orderly point process in time can be uniquely characterized by the joint distribution of the times between successive events-, the number of events in larger time intervals or by its intensity. An elementary example is the Poisson process, where inter-event times are independently exponentially- and the number of events are independently Poisson distributed. The intensity of a Poisson process is constant. A hierarchy of processes with increasing complexity can be found in theory [Cox and Isham, 1980], [Daley and Vere-Jones, 1988] and in applications [Snyder and Miller, 1991], [Lindsey, 2004].

Operations on Point processes

Three types of events disturb the planned schedules: cancellation, delay and pop-up. These three events transform the planned process $\{\tau_i\}, 1 \leq i \leq n$ into the observed process $\{\tau'_j\}, 1 \leq j \leq m$. This can be formalized by the following operations

- $\{\tau_1, \dots, \tau_n\} \rightarrow \{\tau_{t_1}, \dots, \tau_{t_m}\}, m \leq n$ (**thinning**)
some of the events in the planned process are deleted
- $\{\tau_1, \dots, \tau_n\} \rightarrow \{\tau_1 + \epsilon_1, \dots, \tau_n + \epsilon_n\}$ (**random translation**)
individual events are shifted to new locations
- $\{\tau_{1_1}, \dots, \tau_{1_{n_1}}\}, \dots, \{\tau_{k_1}, \dots, \tau_{k_{n_k}}\} \rightarrow \bigcup_{i=1}^k \{\tau_{i_1}, \dots, \tau_{i_{n_i}}\}$ (**superposition**)
 k separate processes are merged

These are standard operations on Point processes [Cox and Isham, 1980], [Daley and Vere-Jones, 1988], [Snyder and Miller, 1991]. Two categories of results exist. The first includes properties of the transformed process, while the second covers limiting results. In general, independence assumptions of the operations underlie these results. Cases of dependent thinning can be found in

[Cox and Isham, 1980] and of dependent random translation in [Snyder and Miller, 1991].

Plan of the section

We first introduce basic notions of point processes and some known results. We then present our results; analytical and experimental. The section closes with interpretation of the results.

Definition A *temporal point process* is a random process whose realizations consist of events $P = \{\tau_i\}, \tau_i \in \mathbb{R}, i \in \mathbb{Z}$.

Definition Let $A \subseteq \mathbb{R}$.

$$N(A) = \text{card}(\{\tau \mid \tau \in A, \tau \in P\})$$

is the number of points in A of a point process P .

Definition Let $A + t = \{x + t : x \in A\}$. A point process is *stationary* if

$$P(N(A_i); i = 1, \dots, k) = P(N(A_i + t); i = 1, \dots, k), \quad \forall t, \forall k = 1, 2, \dots$$

where $A_i \subseteq \mathcal{B}_{\mathbb{R}}$, the Borel tribe on \mathbb{R} .

Definition A point process is *orderly* if

$$P(N(t, t + \delta) > 1) = o(\delta), \quad \forall t \in \mathbb{R}$$

Definition The *rate* of a point process is

$$\rho_t = \lim_{\delta \rightarrow 0^+} \frac{\mathbf{E}(N(t, t + \delta))}{\delta}$$

Definition Let P and P' be two Point processes.

$$\mathbf{E}(N(\cdot)') \mid N(\cdot) = k) = \sum_{l=0}^{\infty} l \cdot P(N(\cdot)' = l \mid N(\cdot) = k)$$

is called the *conditional expectation of process P' given P* .

Proposition 4.2.1 (Thinning) Let P be a stationary, orderly point process with rate λ . Let p be the probability that a point in P is deleted. Then the resulting point process has rate $p\lambda$.

Proposition 4.2.2 (Random Translation) Let P be a stationary, orderly point process with rate λ . Let $P' = \{\tau_i + \epsilon_i\}$ be a random translation with independently, identically distributed random variables ϵ_i . Then P' has unchanged rate λ .

Proposition 4.2.3 (Superposition) Let P_1, \dots, P_k be k independent stationary and orderly point process with rates $\lambda_1, \dots, \lambda_k$. Then the superposition $P = P_1 + \dots + P_k$ has rate

$$\lambda_P = \sum_{i=1}^k \lambda_i$$

The three propositions are classical results and their proof ideas can be found in [Cox and Isham, 1980] or [Snyder and Miller, 1991].

Analytical results

We have results on the impact of random translation on a Poisson arrival process.

Proposition 4.2.4 (Poisson arrival process) *Let $P = \{\tau_i\}$ be a Poisson process with rate λ . Let $P' = \{\tau_i + \epsilon_i\}$ be a random translation of P with disturbances ϵ_i that are (i) independently and (ii) identically distributed with mean μ and variance σ^2 .*

Then the conditional expectation of P' given P is linear in P .

Proof: (sketch) We derive the conditional distribution of the number of arrivals in the disturbed process given the number of arrivals in the planned process and take its expectation:

$$\mathbf{E}(N(\cdot)'|N(\cdot) = k) = kp_S + \lambda(T - b)p_R \quad (4.2)$$

where p_S is the probability of points remaining in the interval $(a, b]$ and p_R is the probability that points in $(b, T]$ enter the interval (see Figure 4.3 for the idea and below for the whole proof).

Bounds

We give bounds for the probabilities p_S and p_R . Let $U_{ab} \sim Unif(a, b)$ and ϵ with $\mathbf{E}(\epsilon) = 0, V(\epsilon) = \sigma^2$ be two independent random variables.

1. From Tchebycheff's inequality follows:

$$p_S = P(U_{ab} + \epsilon \in [a, b]) \geq \frac{2}{3} - \frac{4\sigma^2}{(b - a)^2}$$

For example $P(U_{a,a+5} + \epsilon \in [a, a+5]) \geq 0.1$ for $\sigma^2 > 3$ and $P(U_{a,a+10} + \epsilon \in [a, a+10]) \geq 0.1$ for $\sigma^2 > 15$.

2. From Cramer's inequality follows:

$$p_R = P(U_{bT} + \epsilon \leq b) \leq \frac{1}{4} \frac{(T - b)^2 + 12\sigma^2}{(T - b)^2 + 3\sigma^2}$$

For example $P(U_{b,b+60} + \epsilon \leq b) \leq 0.26$ for $\sigma^2 \in \{0, \dots, 20\}$

□

Proposition 4.2.4 states that systematic gaps between the planned and the realized number of arrivals exist when the only force on the flight schedules is that the arrival times are randomly disturbed. Such gaps would be linear in the number of planned traffic, when the arrival process is Poisson, This is illustrated in the left part of Figure 4.2. It shows the conditional expectation of the disturbed process given the planned process for different values of σ^2 , the standard deviation of the disturbance of an aircraft (dotted lines). The sample

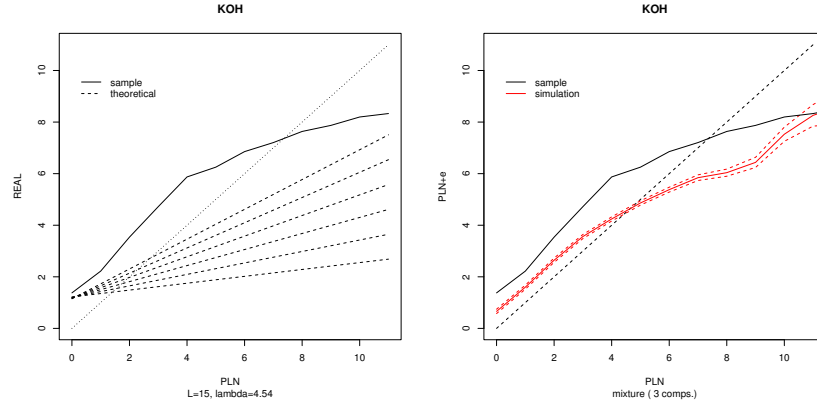


Figure 4.2: Consequences of independence assumption of disturbances $\epsilon_i = \tau'_i - \tau_i$. Left: Poisson process. Right: Flight plans.

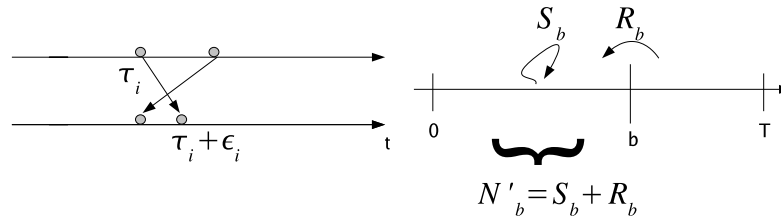


Figure 4.3: Relationship between randomly disturbed Point processes. Left: a planned arrival at time τ_i is translated randomly to $\tau_i + \epsilon_i$. Right: the number of arrivals in interval $(0, b]$ after random translation.

means are plotted in bold. Clearly, such linear functions do not correspond to the sample data. Either the Poisson assumption is wrong, the disturbances ϵ_i are not identically and independently distributed in reality or other forces than random translation act on the system.

Proof of proposition 4.2.4

Figure 4.3 shows the idea. The planned arrival time τ_i of an aircraft is disturbed by some ϵ_i , translating the process P into the process P' (left). For the proof, we are interested in the counting process N'_b of the randomly translated process P' , dependent on the initial process P . For this we need to know the number S_b of aircraft remaining in $(0, b]$ and those R_b that arrive additionally (right).

Let:

1. $P = \{\tau_i\}$ a Poisson process with rate λ (the planned schedule)
2. $P' = \{\tau_i + \epsilon_i\}$ a random translation of P (ϵ_i are i.i.d. random variables with mean μ and variance σ^2 , independent of τ_i).
3. N_{ab}, N'_{ab} : number of arrivals in P, P' in $(a, b]$.
4. $S_{ab} = \text{card}(\{\tau_i + \epsilon_i \in (a, b] \mid \tau_i \in (a, b]\})$: number of arrivals remaining in $(a, b]$
5. $R_{ab} = \text{card}(\{\tau_i + \epsilon_i \in (a, b] \mid \tau_i \geq b\})$: number of arrivals entering $(a, b]$ from the right.
6. U_{ab} : a uniformly distributed random variable in $(a, b]$ (the planned arrival time of an aircraft).

Probability distribution

We derive $\mathbf{E}(N'_{ab} \mid N_{ab} = k)$ as a function of k and σ^2 . Since $N'_{ab} = N'_{0b} - N'_{0a}$ we only need to derive $P(N'_b \mid N_b)$.

$$\begin{aligned} P(N'_b = n \mid N_b = k) &= P(S_b + R_b = n \mid N_b = k) \\ &= \sum_{l=0}^n P(S_b = l, R_b = n - l \mid N_b = k) \end{aligned}$$

since S_b and R_b are independent

$$= \sum_{l=0}^n P(S_b = l \mid N_b = k) P(R_b = n - l \mid N_b = k)$$

and R_b is independent of N_b

$$\begin{aligned} &= \sum_{l=0}^n P(S_b = l \mid N_b = k) P(R_b = n - l) \\ &= \sum_{l=0}^n P(S_b = l \mid N_b = k) \sum_{j=0}^{\infty} P(R_b = n - l \mid N_{bT} = j) P(N_{bT} = j) \end{aligned}$$

Let $p_S = P(U_b + \epsilon \in (0, b])$, $p_R = P(U_{bT} + \epsilon \in (0, b])$. Then

$$\begin{aligned} &= \sum_{l=0}^{\min(n,k)} \binom{k}{l} p_S^l (1 - p_S)^{k-l} \sum_{j=n-l}^{\infty} \binom{j}{n-l} p_R^{n-l} (1 - p_R)^{j-n+l} \frac{\lambda^j (T-b)^j e^{-\lambda(T-b)}}{j!} \\ &= \sum_{l=0}^{\min(n,k)} \binom{k}{l} p_S^l (1 - p_S)^{k-l} \frac{[\lambda(T-b)p_R]^{n-l} e^{-\lambda(T-b)p_R}}{(n-l)!} \end{aligned} \quad (4.3)$$

This is the sum of a *binomial*(p_S, k) and a *Poisson*($\lambda(T-b)p_R$) variable. It follows:

$$\mathbf{E}(N'_b \mid N_b = k) = kp_S + \lambda(T-b)p_R \quad (4.4)$$

Notes

- There is no dedicated point 0 in the aircraft application. It is possible, that points ‘leave’ the interval $(0, b]$ to the left or ‘arrive’ from the left (before midnight). This would lead to $2\lambda p_R$ in (4.3), when the intervals are of equal length (and to $\lambda(T_\lambda - b)p_\lambda + \mu(a - T_\mu)p_\mu$, when the processes and intervals are different). In both cases, the linearity in k of the conditional expectation (4.4) remains.
- The variance of the distribution (4.3) is $kp_S q_S + \lambda p_R$ (the variables are independent). Thus, the distribution is not Poisson. But for high k and low p_S it can be approximated by a Poisson distribution.
- The impact from random rerouting is a simple extension of the results. It corresponds to thinning (cancellations, rerouting) and superposition (arrival of rerouted aircraft), which are linear operations, as shown in propositions 4.2.1 and 4.2.3.

Noise	Agreement $\geq 90\%$	Agreement $\leq 30\%$	Disagreement hd
Gauss	17 %	25 %	74 %
GM	25 %	25 %	78 %

Table 4.1: Simulation results of 12 randomly selected sectors.

Experimental results

We have two results on the impact of random translation on the real flight schedules.

Distribution of the disturbances Figure 4.4 shows the histogram of the disturbances ϵ_i (black). On the left side, a Gaussian distribution is superposed. It is too dispersed and too flat. On the right side, a Gaussian mixture distribution $f(\epsilon) = \sum_{k=1}^3 \pi_k \Phi_k(\epsilon)$ with 3 components is superposed (green). Its parameters are estimated with maximum likelihood, using the expectation-maximization algorithm (EM) [Dempster et al., 1977]. Visibly, the uncertainty around ϵ_i can be characterized by a Gaussian mixture distribution with 3 components. This result is in harmony with background knowledge about the take-off behavior of pilots and with results reported in [Tu et al., 2007]. We do not deepen this result because of the (yet) unknown dependency structure of the process.

Simulation To analyze the impact of random translation on the real flight plans we simulate the model $\tau'_i = \tau_i + \epsilon_i$, where $\{\tau_i\}$ is the planned arrival process and ϵ_i are independently and identically distributed random variables. We assume Gaussian and Gaussian mixture distributions in two separate simulations. The hypothesis is that the disturbances are independently and identically distributed.

The right part of Figure 4.2 shows a typical result. It displays the conditional expectation of the simulated process (y-axis) given the planned process (x-axis). The red curve is the simulation result, where the ϵ_i are drawn from Gaussian mixture distributions. The parameters of the distribution are estimated from $\tau'_i - \tau_i$ by maximum likelihood. Sample size is $n = 3000$. The black curve shows the sample means. The simulation result has a logarithm-like shape. It is similar to the sample means. Agreement between the two profiles is tested with $H_0 : \mu_{s_i} = \mu_i, \forall i$, where μ_{s_i} is the simulated mean value of the number of arrivals under the condition that i have been planned. μ_i is this quantity observed in the data. In the case of Figure 4.2, the hypothesis is rejected in 9 of the 10 cases (5 % level, two-sided). Moreover, the disagreement is larger for high traffic densities ($\text{PLN} \geq 4$).

The general situation is summarized in table 4.1. Simulations of Gaussian and Gaussian mixture random translations are run on twelve randomly selected

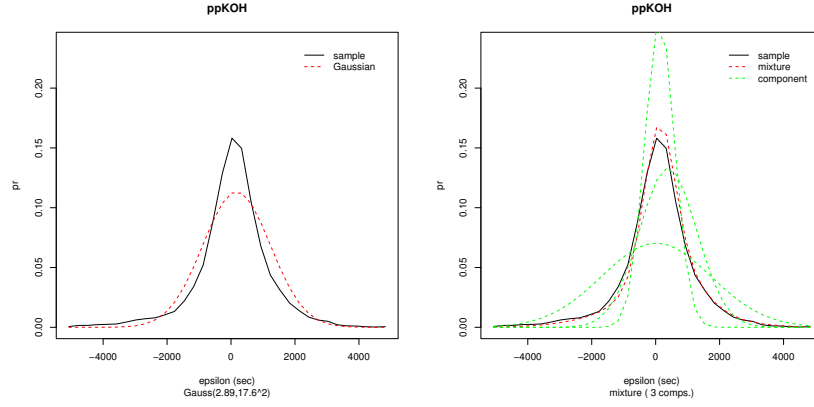


Figure 4.4: Empirical distribution of the disturbances $\epsilon_i = \tau'_i - \tau_i$ (black) and fitted candidates. Left: Gaussian distribution. Right: Gaussian mixture (red) The green distributions are three identified Gaussian components.

sectors. The results of the t-tests are classified by two criteria: agreement $\geq 90\%$ and agreement $\leq 30\%$. Both, for the Gaussian and the Gaussian mixture distributions, $\approx 75\%$ of the sectors have disagreement and 25 % have strong disagreement with the sample data (first and second column). Moreover, the disagreement occurs mainly ($\approx 70\%$) in situations with high traffic densities (third column).

Interpretation

Both, the theoretical and the experimental results state that there are systematic gaps between planned and realized traffic, when the only force on the system is that pilots randomly arrive too late or too early at a sector.

When the arrival process is Poisson, they can be described by a linear function of the traffic density, no matter how the distributions of the random disturbances look like. This is intuitive since the two processes become independent for large σ^2 , and the gaps between them are then described by a horizontal line through $p_R\lambda$. The linearity in this model can be explained by the fact that all terms enter the distribution in additive and constant ways.

When the arrival process is the empirical flight plan, the gap function becomes non-linear. Thus the non-linearity of the observed gaps is partly due to the structure of the arrival process. This is evidence that the Poisson hypothesis is wrong. But still, simulated and observed curves differ significantly from another. This means that either the independence- or the identity assumption are wrong, as well.

We conclude (i) that gaps between planned and realized traffic have to be expected, even when disturbances occur completely at random, (ii) that the logarithm-like shape of the observed gaps is partly due to the structure of the planned arrival process. And (iii), that either the disturbances are not independently and identically distributed in reality or other forces than random translation act on the system.

4.3 Dependency Structure of Disturbances

We have shown that systematic gaps between the number of planned and realized aircraft exist, even when the disturbances of aircraft occur completely at random. We also concluded that either the disturbances are not independently and identically distributed in reality or other forces than random translation act on the system. In this section we report our results on the dependency structure of the disturbances $\{\epsilon_1, \dots, \epsilon_n\}$.

Flow structure

Typically, aircraft from different parts of the airspace arrive at an en-route sector. For example, aircraft A has crossed a congested region. Or aircraft B started at a congested airport. Both will be deviated from their flight plans. In general, there are many aircraft types and many types of uncertainty.

One way to proceed is to analyze sub-processes $\{\epsilon_{c_1}, \dots, \epsilon_{c_n}\}$ where c is a particular traffic condition. For example [Wanke et al., 2004] analyze delay distributions under several traffic conditions. The aggregation of such results can be analyzed asymptotically [Cox and Isham, 1980] or experimentally in Monte-Carlo simulations. The advantage of this approach is that it results in a realistic physical model of the arrival flows. The disadvantages are that many variables have to be considered and that interaction between individual processes has to be considered separately. Such interactions are important, because they are, beside others, induced by the air-traffic controllers. Currently, modeling the human component in air-traffic flow planning is an open research question [Wanke et al., 2005].

Another way to proceed is to describe the sequences $\{\epsilon_1, \dots, \epsilon_n\}$ directly. This summarizes the impact of all uncertainty components on the planned arrival time of an aircraft. Presented in a compact form, it gives insight in the uncertainty in flow planning. The disadvantage is that no causal interpretation can be expected from this analysis. For example, correlation between the the disturbances of successive flights A and B from flows under different traffic conditions does not imply that delay of aircraft A causes delay of aircraft B. However, it can be assumed that unsystematic effects disappear with a sufficiently large amount of data.

We have results for the second approach; dependency patterns in the autocorrelation function that occur in every en-route sector.

Exponentially and polynomially decaying autocorrelation

The correlogram, the plot of the estimated autocorrelation between x_t and x_{t-k} against k is a standard tool for describing linear properties of a single series. In many cases, a decaying pattern of coefficients can be observed

[Granger and Ding, 1996].

A class of models with exponentially decaying autocorrelation are autoregressive models

$$y_t = \sum_{i=1}^{\infty} \phi_i y_{t-i} + a_t$$

A special case is the first-order autoregressive model AR(1)

$$y_t = \phi y_{t-1} + a_t$$

where y_t is a zero mean process and a_i are i.i.d random variables with mean $\mu = 0$ and variance σ^2 .

Its variance is

$$\begin{aligned} \mathbf{E}(y_t^2) &= \phi^2 \mathbf{E}(y_{t-1}^2) + \mathbf{E}(a_t^2) + 2\phi \mathbf{E}(y_{t-1} a_t) \\ &= \frac{\sigma^2}{1 - \phi^2} \\ &= \gamma(0) \end{aligned}$$

because a_t is independent from y_{t-k} by definition. This implies that

$$1 - \phi^2 > 0 \quad \text{or} \quad |\phi| < 1$$

because a variance has to be strictly positive. The covariance at lag k is

$$\begin{aligned} \mathbf{E}(y_t y_{t-k}) &= \phi \mathbf{E}(y_{t-1} y_{t-k}) + \mathbf{E}(a_t y_{t-k}) \\ &= \phi \gamma(k-1) \end{aligned}$$

Dividing by $\gamma(0)$ leads to the autocorrelation function

$$\begin{aligned} \rho(k) &= \phi \rho(k-1) \\ &= \phi^k \end{aligned}$$

The exponentially decaying autocorrelation is a typical characteristic of Markov processes [Cox and Miller, 1977] and more generally of many stationary ARMA processes [Granger and Ding, 1996]. This is because of the carry-over effect: when y_t is highly correlated with y_{t-1} , then it is also correlated with y_{t-k} .

There are several classes of models with non-exponentially decaying autocorrelation. For example, processes with linear mean show slowly declining sample autocorrelations. Other classes are ‘long memory models’ [Granger and Ding, 1996]. Their autocorrelations decline at a slower rate than ARMA models. Examples are fractionally integrated models and certain non-linear models [Granger and Ding, 1996].

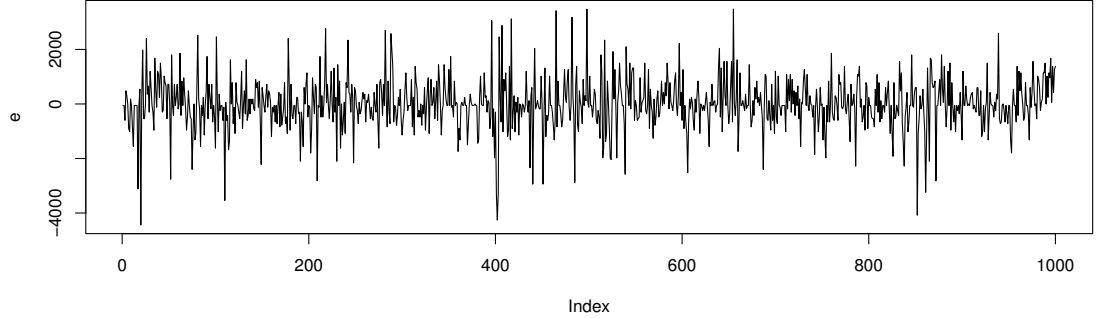


Figure 4.5: Time plot of the disturbances ϵ_i .

Dependency structure of disturbances

Figure 4.5 shows the time plot of the disturbances ϵ_i . The mean seems to increase and decrease in periods of 30 units. No global time trend is visible. The variance is constant over time.

The upper part of Figure 4.6 shows sample autocorrelation and partial autocorrelation of the disturbances ϵ_i . Autocorrelations start at ≈ 0.1 and decay slowly until lag 40. The partial autocorrelations decay until lag 15. Interpretation is difficult, non-stationarity in the mean may cause spurious coefficients.

The lower part of Figure 4.6 shows sample autocorrelation and partial autocorrelation of the first difference of the disturbances $\nabla\epsilon_i = \epsilon_i - \epsilon_{i-1}$. A single peak of -0.49 at lag 1 of the acf and an exponentially decaying pattern in the pacf can be seen. This is the characteristics of an IMA(1,1) process: $\epsilon_i = a_i + (\epsilon_{i-1} - \theta a_{i-1})$ with a_i i.i.d. random variables. An interpretation is that random events (e.g. weather conditions at departure airport) cause a delay a_i of aircraft i and (very weakly) of its successor $i - 1$.

But there is no justification to difference the data because no linear trend and no random walk can be assumed a priori. A possible explanation is an autoregressive dependency close to 1. To analyze this we pose the ARMA(1,1) model:

$$\epsilon_i = \phi\epsilon_{i-1} + \theta a_{i-1} + a_i \quad (4.5)$$

with a_i i.i.d. random variables. For $\phi = 1$, the special case IMA(1,1)

$$\nabla\epsilon_i = \theta a_{i-1} + a_i \quad (4.6)$$

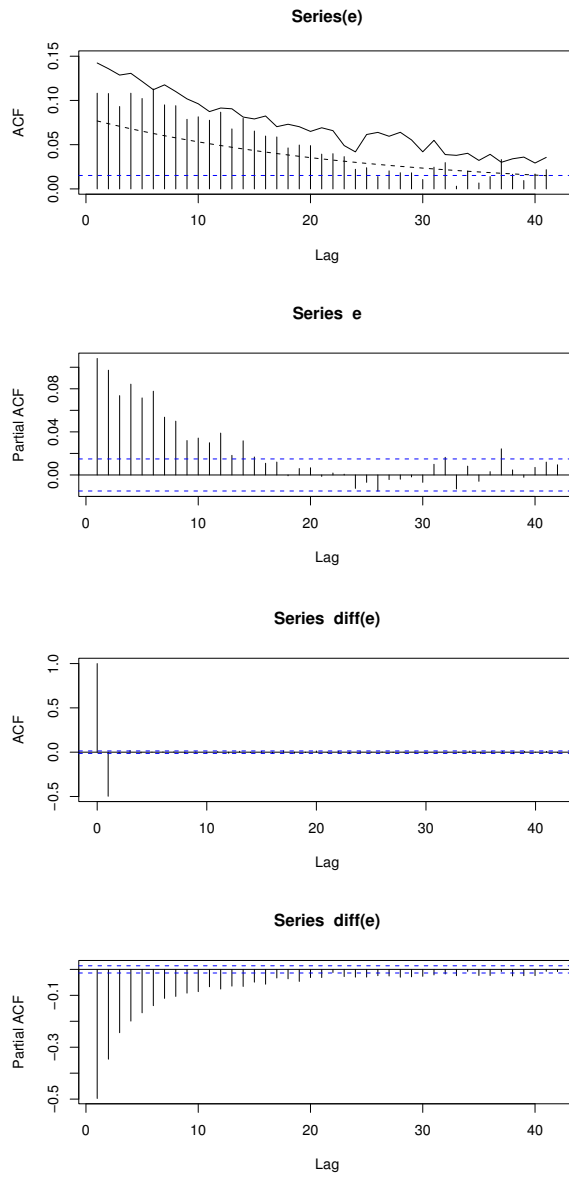


Figure 4.6: Sample autocorrelation and partial autocorrelation plots. Left: ϵ_i . Right: $\nabla\epsilon_i = \epsilon_i - \epsilon_{i-1}$

arises.

The autocovariance function of the ARMA(1,1) is

$$\gamma(k) = \phi\gamma(k-1), \quad k \geq 2$$

It behaves like that of an AR(1) scheme after the first lag. The IMA(1,1) is non-stationary; the autocovariance is not a function of the lag k . There are results that show that it decays polynomially in the lag k [Kendall et al., 1983]. ARMA(1,1) and IMA(1,1) models are applied in industrial control, where the impact of random disturbances on the production scheme is studied [Box and F.Jenkins, 1970]. Our analysis is exploratory; we do not have a priori arguments for neither of the models. However, a direct interpretation for model 4.5 is that a delayed aircraft is followed by a delayed aircraft. Moreover, external events disturb i and its successor. On the other hand, due to duality results, an ARMA(1,1) model represents a large class of processes. Interpretation can become ambiguous [Kendall, 1989].

Table 4.2 compares the fit of an IMA(1,1) model with an ARMA(1,1) model to our data. The parameters are obtained by exact maximum likelihood estimation. In the ARMA model, the AR parameter ϕ is close to 1 but significantly different from it. The MA-parameter θ is -0.88. There is also a mean value μ estimated (not shown). The variance of the unexplained part a_i is 18.1² min. For the IMA model, the MA parameter is -0.94. No mean is included in the model. The estimated variance of the unexplained series a_i is 18.24² min. The AIC of the ARMA model is lower than for the IMA model, despite the larger number of parameters. Table 4.3 compares the AIC for eight randomly selected sectors. The ARMA has always a lower AIC than the IMA (last column). But the main argument against the IMA model is that differencing does not make sense physically. Table 4.4 shows the maximum likelihood estimates of the eight ARMA models. The autoregressive component is always close to 1 but never significantly equal to 1. The moving average component is always negative and always < -0.8 . Coming back to the autocorrelation in the upper panel of Figure 4.6, we plot the theoretical (dotted) and the simulated (bold) autocorrelation function of the estimated ARMA model. The global pattern of decay is captured by both whence a step at lag 23 and a peak at lag 37 may need some more interpretation. Figures 4.8 and 4.9 show diagnostic plots for the ARMA model. The residuals contain no trend and no autocorrelation. The normality assumption, however, cannot be justified. Table 4.4 contains the parameter estimations for eight randomly selected sectors. The autoregressive parameter is always close to 1 and the moving-average parameter is always negative.

To better understand this result we look at sequences of correlated deviations. A simple pattern would be that long sequences of correlated disturbances exist. This could be interpreted by events at departure airports that affect several aircraft (e.g. runway congestion). Figure 4.7 shows the distribution of the

Name	Model	ϕ	θ	σ^2	AIC
ARMA	$\epsilon_i = \phi\epsilon_{i-1} + \theta a_{i-1} + a_i$	0.96 (0.005)	-0.88 (0.007)	18.11	291884.4
IMA	$\epsilon_i = \epsilon_{i-1} + \theta a_{i-1} + a_i$	1	-0.94 (0.004)	18.24	292110.1

Table 4.2: Comparison ARMA(1,1) and IMA(1,1).

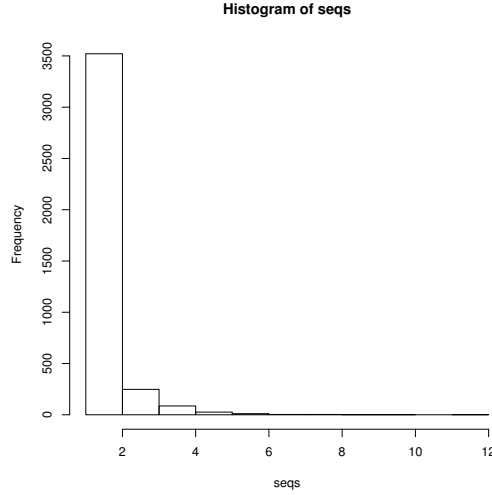


Figure 4.7: Distribution of the lengths of sequences with correlated arrivals.

lengths of correlated sequences. There are rarely more than two successively correlated arrivals and never more than 6. Thus the arrival patterns are heterogeneous. This is the same for sectors with only one arrival route and for more complex sectors. This has to be analyzed in more detail.

We conclude that the disturbances ϵ_i are not independent in reality. Their dependencies show similar second-order characteristics than IMA(1,1) and ARMA(1,1) models. However, these findings are empirical and both models cannot be justified a priori.

4.4 Interpretation

The analysis of consequences of independence assumptions (section 4.3) shows that systematic gaps between planned and observed counting processes are to be expected, when disturbances occur completely at random. When the planned process is Poisson, these gaps can be described by a linear function of the counting process, no matter how the distributions of the random disturbances look like. This is intuitive since the two processes become independent for large σ^2 ,

Sector	ARMA	IMA	ARMA – IMA
LUE	362352.6	362517.2	-164.7
CLW	327350.0	327566.1	-216.1
EXN	298291.4	298376.9	-85.5
EUY	369497.8	369636.7	-138.9
L UW	355430.6	355586.6	-156.0
KOH	311295.4	311500.8	-205.4
NIH	402112.7	402317.4	-204.8
LNH	327560.6	327738.7	-178.0

Table 4.3: AIC for ARMA(1,1), IMA(1,1) and their difference for eight randomly selected sectors.

Sector	ϕ	θ	μ	σ^2	loglik	AIC
LUE	0.98 (0.003)	-0.92 (0.005)	0.9 (29.4)	1359967	-171041.9	342091.7
CLW	0.95 (0.005)	-0.88 (0.007)	62.2 (14.6)	813595	-154553.4	309114.9
EXN	0.97 (0.003)	-0.92 (0.006)	196.3 (21.8)	766710	-141918.0	283844.0
EUY	0.98 (0.002)	-0.93 (0.004)	204.0 (21.1)	781522	-176817.1	353642.2
L UW	0.97 (0.003)	-0.91 (0.005)	150.7 (27.6)	151341	-166914.3	333836.5
KOH	0.96 (0.005)	-0.88 (0.007)	89.5 (21.2)	1181206	-145938.2	291884.4
NIH	0.97 (0.003)	-0.90 (0.005)	102.1 (21.0)	1034263	-188931.2	377870.5
LNH	0.96 (0.004)	-0.88 (0.006)	69.8 (22.2)	1061602	-150761.3	301530.5

Table 4.4: Validation ARMA(1,1) for eight randomly selected sectors.

and the gaps between them are then described by a horizontal line through $p_R\lambda$. The linearity in this model can be explained by the fact that all terms enter the distribution in additive and constant ways. When the planned process is the empirical flight schedule, the gap function becomes non-linear. Thus the non-linearity of the observed gaps is partly due to the structure of the arrival process.

The data analysis (section 4.3) shows that dependencies between the disturbances of successive flights exist in reality. We identified two linear time-series models with similar second order structure. However, an arrival flow consists of aircraft from different origins and of different types. Moreover, the correlation structure shows that the correlation last up to $\approx 2h$. A possible interpretation is that delayed aircraft keep their delay on their way back. All this suggests that the data consists of superpositions of different processes. This has to be analyzed in more detail before justifying a data generating mechanism.

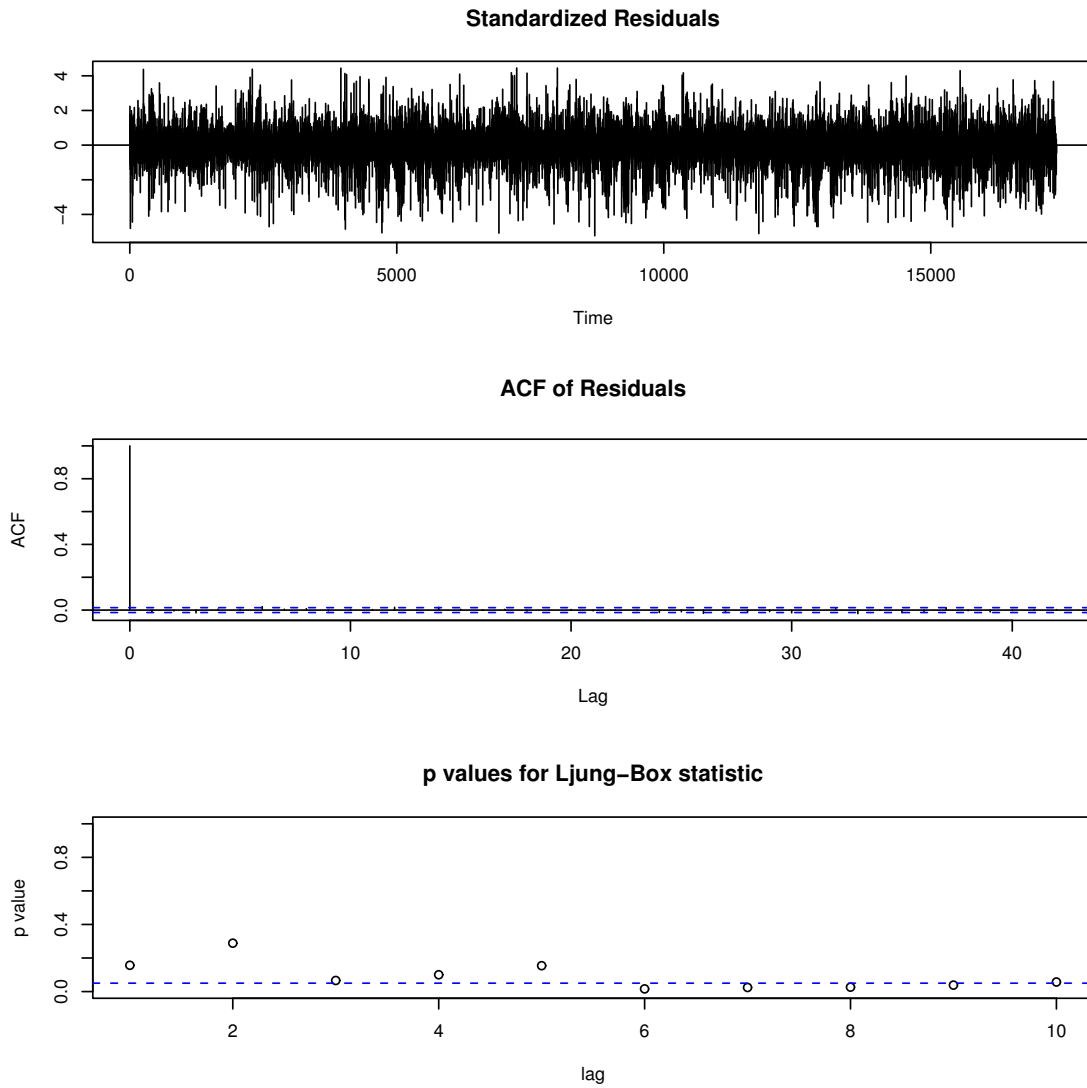


Figure 4.8: Diagnostics for the ARMA(1,1) model $\epsilon_i = 0.96\epsilon_{i-1} + -0.88a_{i-1} + a_i$. Top: residual time plot. Middle: acf of the residuals. Bottom: p-values for the portmanteau test.

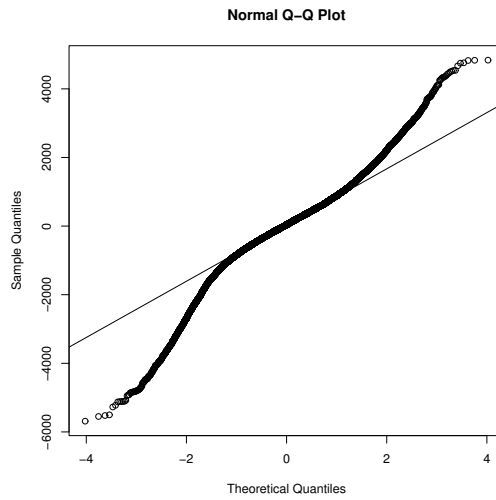


Figure 4.9: QQ plot of the ARMA(1,1) residuals. The tails do not correspond with a Gaussian distribution.

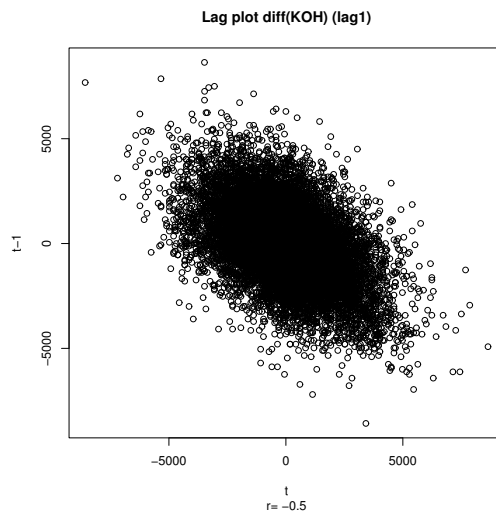


Figure 4.10: Lag plot for $\nabla \epsilon_i = \epsilon_i - \epsilon_{i-1}$ at lag 1.

Chapter 5

Conclusions and Future Work

Uncertainties are ubiquitous in air traffic-management. While their sources are widely known (demand-, capacity-, and flow control uncertainties), their impact on its components is less well understood. In this thesis we analyzed past radar data in order to better understand the mechanisms that lead to gaps between the predictive and the adaptive components in air-traffic management. The analysis is exploratory with the purpose of gaining insight in the causal mechanisms that lead to gaps. In particular, we did not build a model but we analyzed aspects of the phenomenon. We believe that the results are useful in understanding the impact of uncertainties in current flow planning. Based on this, a realistic model can be built to optimize the network resources.

5.1 Summary of contributions

This thesis contributes to the field of ‘uncertainties in air traffic flow planning’ and to the discussion about the role of algorithms in an analysis of data. Our contributions have been presented at national and international conferences in the domains ‘operations research’ and ‘transportation systems’ [Gwiggner et al., 2004], [Gwiggner, 2004], [Gwiggner and Lanckriet, 2004], [Gwiggner et al., 2005], [Gwiggner and Duong, 2006], [Föll and Gwiggner, 2006] and submitted to an international journal [Gwiggner, 2007]. They are divided into three parts.

Gaps between predictive and adaptive component The main discoveries are that there are *systematic* gaps in every sector of the airspace and that the size of these gaps can be characterized by Poisson distributions. In average more than planned aircraft arrive when few are planned and less when many are planned. This is counter-intuitive because one expects that the different uncertainty factors cancel out in average [Gwiggner and Duong, 2006]. We then analyze the hypothesis that the observed gaps are due to *random disturbances*

on flight schedules. Based on stochastic Point processes we prove that pure random disturbances of the planned entry times cause systematic gaps in three classes of flight schedules. But we also show that the observed gaps are only *partly* explainable by pure random disturbances [Gwiggner, 2007]. From this we conclude (i) that even if all controllable uncertainties in flow planning were eliminated, systematic gaps between the number of planned and realized traffic would remain and (ii) that the disturbances are not independent in reality. This result is useful in tactical flow planning. New constraints in the slot-allocation procedure can be found by identifying classes of flight schedules that are robust to random disturbance.

Propagation of uncertainties We have two results concerning the propagation of uncertainties through the sector network: Firstly, an analysis of the sample correlation matrix function of the most congested part of the airspace suggests that gaps propagate exclusively on flight routes. The higher the traffic density is, the longer the propagation takes place. No unexpected correlation is identified. This is evidence that no systematic re-routing is initiated by controllers to absorb gaps [Gwiggner et al., 2004], [Gwiggner et al., 2007]. Secondly, gaps of flights show time dependencies up to 2h. Moreover, the probabilities in the tails and around the center of the distributions of gaps are higher than for standard distributions. We identify three time-series models with similar second-order characteristics. This is evidence for heterogeneous behavior of flights and that reactionary delays have an impact on the workload at en-route sectors. But the result is empirical and we conjecture that it is due to aggregation and long-range dependence at the en-route sector level.

Algorithms in data analysis Recently an algorithmic approach to analyze high-dimensional data sets became popular [Breiman, 2001], [Hastie et al., 2003]. Compared to traditional statistical techniques, it contributes to the prediction problem but it is criticized to lead to uninterpretable results [Cox, 2001], [Efron, 2001], [Saporta, 2006]. We experience some of the well-known limitations of data-driven approaches e.g. the problem of trend-removal or the ambiguity of second-order characteristics in time-series models and conclude that when the purpose of an analysis is interpretation, the priority is ‘to ask the right questions’ and not to apply sophisticated prediction algorithms [Gwiggner, 2005]. This thesis contributes a concrete example to the discussion of the role of algorithms in an analysis of data.

5.2 Perspectives

The main results of the thesis are (i) that even if all controllable disturbances in flow planning were eliminated, systematic gaps between the number of planned and realized traffic would remain and (ii) that the disturbances are not independent in reality. This motivates future work in the following directions:

Statistical model of gaps: Tails in marginal distributions and long-range dependencies (sections 3.2 and 4.3) are signs that real traffic consists of heterogeneous groups and that reactionary delays have an impact on en-route sector workload. As next step we propose to further dis-aggregate the data to isolate the different groups and to analyze the phenomenon of delay-propagation (reactionary delay) in more detail. This is the basis to quantify the impact of local decisions (e.g. at airports or in flow management centers) on the performance of the global sector network. Similar phenomena can be observed in the analysis of telecommunication networks [Baccelli, 2002], [Cappé et al., 2002].

Robust flow optimization: We identified two classes of schedules in which random disturbances cause systematic gaps (section 4.2). We propose to continue this theoretical analysis in order to identify classes of flight schedules that absorb the impact of uncontrollable random disturbances. Inspirations can be found in the thesis of [Ferchaud, 2006] and in percolation theory (*‘how do flows propagate in a stochastic medium?’*) [Grimmett, 1999], [Amor et al., 2006].

Bibliography

- E. Aarts and L.K. Lenstra. *Local Search in Combinatorial Optimization (editors)*. Wiley, Chichester, England, 1997.
- E. Altman and L. Wynter. Equilibrium, games and pricing in transportation and telecommunication networks. *Networks and Spatial Economics*, 4:7–21, 2004.
- S. B. Amor, M. Bui, and I. Lavallée. A Complex Systems Approach in ATM Modeling. In *European Conference on Complex Systems, ECCS 06, Oxford*, 2006.
- T.W. Anderson. *An Introduction to Multivariate Statistical Analysis*. Wiley, 1958.
- F. Baccelli. Internet: Modéliser le trafic pour mieux le gérer. In Société de mathématique de France (SMF) et Société de mathématiques appliquées et industrielles (SMAI), editor, *l'Explosion des mathématiques*, pages 75–79. Ecole polytechnique, Palaiseau, 2002.
- M.O. Ball, D. Lovell, R. Hoffman, and A. Mukherjee. Response mechanisms for dynamic air traffic flow management. In *Proceedings of the 6th Europe-USA ATM Seminar. Baltimore. US.*, 2005.
- M.S. Bartlett. *Probability, Statistics and Time*. John Wiley and Sons, 1975.
- A. Bayen, R. Raffard, and C. Tomlin. Adjoint-based control of a new Eulerian network model of air traffic flow. *IEEE Transactions on Control Systems Technology*, 14(5), 2006.
- N. Boghadi. Modeling demand uncertainties during ground delay programs. Technical report, University of Maryland, 2002.
- G. Box and F. Jenkins. *Time Series Analysis. Forecasting and Control*. Holden-Day, San Francisco, 1970.
- S. Boyd and L. Vandenberghe. *Convex Optimization*. Cambridge University Press, Cambridge, 2004.

- L. Breiman. Two cultures in statistical modelling. With discussion. *Statistical Science*, 16-3, 2001.
- D. R. Brillinger and A.E.P. Villa. Assessing connections in networks of biological neurons. In L. T. Fernholz D. R. Brillinger and S. Morgenthaler, editors, *The Practice of Data Analysis: Essays in Honor of John W. Tukey*, pages 77–92. Princeton Univ. Press, Princeton, 1997.
- D.R. Brillinger. Remarks concerning graphical models for time series and point processes. *Brazilian Review Econometrics*, 16:1–23, 1996.
- Peter Bühlmann. Bootstraps for Time Series. *Statist. Sci*, 17(1):52–72, 2002.
- A.C. Cameron and P.K. Trivedi. *Regression Analysis of Count Data*. Cambridge University Press, Cambridge, UK, 1998.
- O. Cappé, E. Moulines, J-C. Pesquet, A. Petropulu, and Z. Yang. Long-range dependence and heavy-tail modeling for teletraffic data. *IEEE Signal Processing Magazine*, 19(3):14–27, 2002.
- A.F. Chalmers. *What is this thing called science ? An assesment of the nature and status of science and its methods*. University of Queensland Press, 1982.
- S. K. Chatterjee. *Statistical Thought. A Perspective and History*. Oxford University Press, 2003.
- S. Constans, E. Faouzi, O. Goldschmidt, and R. Fondacci. Optimal flight level assignment: introducing uncertainty. *Proceeding of the 4th INO Workshop*, 2004.
- D.R. Cox. Role of models in statistical analysis. *Statistical Science*, 5:169–174, 1990.
- D.R. Cox. Reply to: L. Breiman. Two cultures in statistical modelling. With discussion. *Statistical Science*, 16-3, 2001.
- D.R. Cox. *Principles of Statistical Inference*. Cambridge University Press, 2006.
- D.R. Cox and V. Isham. *Point Processes*. Chapman and Hall, 1980.
- D.R. Cox and H.D. Miller. *The theory of stochastic processes*. Chapman and Hall/CRC, 1977.
- D.R. Cox and E.J. Snell. *Applied Statistics - Principles and Examples*. Chapman and Hall/CRC, 1981.
- D.R. Cox and N. Wermuth. *Multivariate Dependencies. Models, Analysis and Interpretation*. Chapman and Hall/ CRC, 1998.
- D.J. Daley and D. Vere-Jones. *An Introduction to the theory of Point Processes*. Springer, 1988.

- A.P. Dempster, N.M Laird, and D.B. Rubin. Maximum likelihood from incomplete data via the em algorithm. *Journal of the Royal Statistical Society. Series B*, 39:1–22, 1977.
- P.J. Diggle. *Time Series: A Biostatistical Introduction*. Oxford University Press, 1990.
- A. W. F. Edwards. *Likelihood*. Cambridge University Press, New York, 1972.
- B. Efron. Reply to: L. Breiman. Two cultures in statistical modelling. With discussion. *Statistical Science*, 16-3, 2001.
- EUROCONTROL. *Revised Convention*. EUROCONTROL, 1997.
- EUROCONTROL. Independent Report for the Improvement of ATFM. *Euro-control*, 2002.
- EUROCONTROL. Cosaac User Manual. Release 3.9.3. Technical report, EEC, 2004.
- EUROCONTROL. *EEC Activity Report 2005*. EUROCONTROL, 2005.
- EUROCONTROL. *Performance Review Report 2005*. EUROCONTROL, Brussels, Belgium, 2006.
- L. Fahrmeir and G. Tutz. *Multivariate statistical modelling based on generalized linear models. 2nd edition*. Springer, New York, 2001.
- F. Ferchaud. Etude des zones d’absorption pour la gestion de flux du trafic aérien. *PhD Thesis. Université de Bordeaux*, 2006.
- B. Pesic Le Foll and C. Gwignier. Possible model to highlight interdependencies between flow regulations. In *Proceedings of the 2nd International Conference on Research in Air Transportation. ICRAT 2006*, Belgrad, Serbia, 2006.
- N. H. Gartner, C. Messer, and A. Rathi. *Traffic Flow Theory. A revised State of the Art Report*. Transportation Research Board (TRB) Special Report, <http://www.tfhrc.gov/its/tft/tft.htm>, 2002.
- D. Gazis. *Traffic Theory*. Springer. International Series in Operations Research & Management Science, 2002.
- P. Giot. Time transformations, intraday data, and volatility models. *Journal of Computational Finance*, 4/2:31–62, 2001.
- C.W.J. Granger and Z. Ding. Varieties of long memory models. *Journal of Econometrics*, 73:61– 77, 1996.
- W. H. Greene. *Econometric Analysis*. Prentice Hall, 5th edition, 2002.
- P. Grimmett. *Percolation*. Springer, 1999.

- R. Guerreau. FAM. *Eurocontrol. Technical Report.*, 2000.
- C. Gwiggner. Implicit relations between time slots, capacity and real demand in ATFM. In *Proceedings of the 23rd IEEE Digital Avionics Systems Conference. DASC 2004*, Salt Lake City, U.S.A. IEEE Press, 2004.
- C. Gwiggner. An Opinion on Data Mining. Technical report, LIX, Ecole Polytechnique, 2005.
- C. Gwiggner. Consequences of independence assumptions in ATFM. *Submitted to International Journal of Production Research (IJPR)*, 2007.
- C. Gwiggner, P. Baptiste, and V. Duong. Some spatio-temporal characteristics of the planning error in European ATFM. In *Proceedings of the IEEE Intelligent Transportation Systems Conference. ITSC 2004*, Washington D.C., U.S.A. IEEE Press, 2004.
- C. Gwiggner, P. Baptiste, and V. Duong. Conditions et lois: Une analyse des données du trafic aérien. In *6ème congrès de la Société Française de Recherche Opérationnelle et d'Aide à la Décision. ROADEF*, Tours, France, 2005.
- C. Gwiggner, P. Collet, and J.M. Marion. Propagation of airspace congestion. A vector correlation analysis. *To be submitted*, 2007.
- C. Gwiggner and V. Duong. Averages, Uncertainties and Interpretation in Flow Planning. In *Proceedings of the 2nd International Conference on Research in Air Transportation. ICRAT 2006*, Belgrad, Serbia, 2006.
- C. Gwiggner and G. Lanckriet. Characteristics in flight data - Estimation with logistic regression and Support Vector Machines. In *Proceedings of the 1st International Conference on Research in Air Transportation. ICRAT 2004*, Zilina, Slovakia. Zilina University Press, 2004.
- D. Hand, H. Mannila, and P. Smyth. *Principles of Data Mining*. MIT Press, 2001.
- M. M. Hansen and W. Wei. Multivariate analysis of the impacts of NAS investments: A case study of a major capacity expansion at Dallas-fort worth airport. Technical report, Nextor Research Report, 1999.
- T. Hastie, R. Tibshirani, and J. Friedman. *The Elements of Statistical Learning. Data Mining, Inference, and Prediction*. Springer Series in Statistics, 2003.
- ICAO. *Annual Report of the Council*. International Civil Aviation Organization, 2005. ISBN Doc 9862.
- M.G. Kendall. *Time Series*. Oxford University Press, 3rd edition, 1989.
- M.G. Kendall, A. Stuart, and K. Ord. *The Advanced Theory of Statistics. Volume 3: Design and Analysis, and Time Series. 4th edition*. Charles Griffin & Company Ltd., London, 1983.

- A. N. Kolmogoroff. Grundbegriffe der Wahrscheinlichkeitsrechnung. *Ergebnisse der Mathematik und ihrer Grenzgebiete*, II-3, 1933.
- S.L. Lauritzen. *Graphical Models*. Oxford University Press, 1996.
- O. Ledoit and M. Wolf. A well-conditioned estimator for large-dimensional covariance matrices. *Journal of Multivariate Analysis*, 88-2:365–411, 2004.
- L. Liberti and N. Maculan. *Global Optimization. From Theory to Implementation (editors)*. Springer Verlag, 2006.
- J.K. Lindsey. *Parametric Statistical Inference*. Oxford University Press, 2003.
- J.K. Lindsey. *Statistical Analysis of Stochastic Processes in Time*. Cambridge University Press, 2004.
- A. Majumdar, W.Y. Ochienga, F. McAuley, J.M. Lenzi, and C. Lapatadu. The factors affecting airspace capacity in Europe: A framework methodology based on cross-sectional time series analysis using simulated controller workload. In *Proceedings of the FAA-Eurocontrol ATM2005 Seminar, Baltimore, Maryland, USA*, 2005.
- S. Mallat. *Traitement du signal*. Editions polytechnique, 2000. ISBN 2-7302-0737-6.
- P. K. Menon, G. D. Sweriduk, and K. Bilimoria. New approach for modeling, analysis and control of air traffic flow. In *AIAA Journal of Guidance, Control and Dynamics*, volume 27/5, pages 737–744, 2004.
- A. Mukherjee, D. Lovell, M. Ball, A. Odoni, and G. Zerbib. Modeling delays and cancellation probabilities to support strategic simulations. In *Proceedings of the 6th Europe-USA ATM Seminar. Baltimore. US.*, 2005.
- Y. Pawitan. In *All Likelihood: Statistical Modelling and Inference using Likelihood*. Oxford University Press, 2001.
- J. Pearl. *Probabilistic Reasoning in Intelligent Systems*. Morgan-Kaufmann, 1988.
- C.A. Robelin, D. Sun, G. Wu, and A. M. Bayen. MILP control of aggregate Eulerian network airspace models. *Proceedings of the 2006 American Control Conference*, pages 5257–5262, June 2006.
- G. Saporta. *Probabilités, Analyse des Données et Statistique*. Editions Technip. 2ème edition, Paris, 2006.
- J. Schäfer and K. Strimmer. A shrinkage approach to large-scale covariance matrix estimation and implications for functional genomics. *Statistical Applications in Genetics and Molecular Biology*, 4-1, 2005.

- D.L. Snyder and M.I. Miller. *Random Point Processes in Time and Space, 2nd ed.* Springer-Verlag, New York, 1991.
- B. Sridhar. An aggregate dynamic stochastic model for an air traffic system. In *Fifth International Air Traffic Management R&D Seminar ATM-2003, Budapest, Hungary*, 2003.
- Y. Tu, M.O. Ball, and W. Jank. Estimating flight departure delay distributions—a statistical approach with long-term trend and short-term pattern. In *Forthcoming: Journal of the American Statistical Association*, 2007.
- J.W. Tukey. *Exploratory data analysis*. Addison-Wesley, Massachusetts, 1977.
- C. Wanke, M.B. Callaham, D.P. Greenbaum, and A.J. Masalonis. Measuring uncertainty in airspace demand predictions for traffic flow management applications. *AIAA Guidance, Navigation and Control Conference. Austin, TX, USA.*, 2003.
- C. Wanke, S. Mulgund, D. Greenbaum, and L. Song. Modeling traffic prediction uncertainty for traffic management decision support. *AIAA Guidance, Navigation and Control Conference. Providence RI*, 2004.
- C. Wanke, L. Song, S. Zobell, D. Greenbaum, and S. Mulgund. Probabilistic congestion management. *Proceedings of the 6th Europe-USA ATM Seminar. Baltimore. US.*, 2005.
- J. Whittaker. *Graphical Models in Applied Mathematical Multivariate Statistics*. Wiley, New York, 1990.
- L. Zadeh. Fuzzy sets. *Information and Control*, 8:338–353, 1965.
- L. Zadeh. Fuzzy sets as the basis for a theory of possibility. *Fuzzy Sets and Systems*, 1:3–28, 1978.